AN *IN VITRO* STUDY OF HUMAN FIBROBLAST CONTRACTILITY AND THE DIFFERENTIAL EFFECT OF TGF-β1 AND TGF-β3 ON FIBROBLAST CONTRACTION AND COLLAGEN SYNTHESIS

by

Brian H. Campbell

B.S. in Biological Science at the University of Pittsburgh, 2000

Submitted to the Graduate Faculty of

the School of Engineering in partial fulfillment

of the requirements for the degree of

Master of Science in Bioengineering

University of Pittsburgh

2002

COMMITTEE SIGNATURE PAGE

James H-C. Wang, Ph.D.
Advisor

_____
Signature

ABSTRACT

AN *IN VITRO* STUDY OF HUMAN FIBROBLAST CONTRACTILITY AND THE DIFFERENTIAL EFFECT OF TGF-b 1 AND TGF-b 3 ON FIBROBLAST CONTRACTION AND COLLAGEN SYNTHESIS

Brian H. Campbell, M.S.

University of Pittsburgh

Skin, tendons, and other tissues can heal, but with formation of scar tissue, characterized by altered biochemical composition, distorted tissue architecture, and decreased mechanical properties compared to the normal tissues. Excessive cellular contraction in wounds can lead to formation of scar tissue, whereas insufficient cellular contraction may impede wound closure. In addition, although both TGF-β1 and TGF-β3 have been found to increase cellular contraction, only TGF-β3 has been shown to reduce formation of scar tissue in rat skin wounds. Therefore, the overall objective of this project is to reduce the formation of scar tissue by regulating cellular contraction. As part of this objective, this thesis project studies human fibroblast contractility

and the differential effect of TGF-β1 and TGF-β3 on human fibroblast contraction and collagen synthesis using *in vitro* models. Either human skin or tendon fibroblasts were used in this project, depending on the nature of the specific study.

Human tendon fibroblasts were found to contract *in vitro* and the degree of contraction was dependent on serum concentration. Further, a multi-station culture force monitor (CFM) system was developed to characterize cellular contraction. Using this system, human tendon fibroblasts were found to have a significantly lower maximum contraction force and a markedly different contraction pattern than human skin fibroblasts, illustrating the ability of this system to differentiate between cells from different tissues. In addition, the effect of TGF-β1 and TGF-β3 on cellular contraction and collagen synthesis of human skin fibroblasts was studied using the CFM system. Both TGF-β1 and TGF-β3 were found to increase human fibroblast contraction and collagen synthesis, but TGF-β3 increased cellular contraction and collagen synthesis to a lesser extent than TGF-β1.

As there is great interest in improving the quality of healing tissue, these studies provide a foundation to further study the cellular and molecular mechanisms of tissue wound healing. In addition, these findings suggest that TGF-β3 instead of TGF-β1 may be applied to regulate tendon fibroblast contraction, which may reduce formation of scar tissue in healing tendons. Future studies will continue to elucidate the relationship between cellular contraction and collagen synthesis.

DESCRIPTORS

Cellular Contraction

Collagen Synthesis

Human Patellar Tendon Fibroblasts

Human Skin Fibroblasts

Multi-Station Culture Force Monitor System

Transforming Growth Factor-β1

Transforming Growth Factor-β3

ACKNOWLEDGEMENTS

Throughout the past two years, many people have contributed to the completion of my graduate studies. I will be forever grateful for the guidance and support that Dr. James H-C. Wang, my advisor, provided to me during my past two years of graduate study. I truly admire his dedication and willingness to help, tributes which undoubtedly contributed to the success of my thesis project. I am also very thankful to Dr. Savio L-Y. Woo, director of the MSRC, for his willingness to serve on my committee and his many insightful comments and suggestions throughout my thesis studies. He is a world renowned researcher from whom I have learned the art of research and the philosophies of life. I am also very fortunate to have Dr. Patricia A. Hebda on my committee, whose expertise in wound healing and molecular biology was a great contribution to my understanding and the development of my thesis.

There are many others that I also wish to thank that have helped me throughout the last couple of years. I owe a special thanks to Dr. Harvey Borovetz for his continuous support throughout my undergraduate and graduate studies; I am truly grateful for his friendship. Fengyan Jia is an amazing person who taught me everything about cell culturing, but who I will always remember for her kindness, hard work, and personal values. Tom Gilbert and I started around the same time in the lab, and we learned many things together, but it is the friendship that arose from our working together that I value most. I'd also like to that all the members of the MSRC for their support, keep up the great work!

Most importantly, I'd like to thank my family for all their love and support. Mom and dad, thanks for everything that you've taught me, as well as all the support you've given me throughout my life. Eric and Kim, you are not only my brother and sister, but my best friends; I can't imaging growing up without you! Shanon and Luke, although you are the newest members of our family, I feel that you've always been there and I can't wait for the many years to come! To all of you, thank you, and I love you very much.

TABLE OF CONTENTS

Page

ABSTRACT ..... **iii**

ACKNOWLEDGEMENTS ..... **vii**

TABLE OF CONTENTS ..... **viii**

LIST OF FIGURES ..... **xi**

NOMENCLATURE ..... **xiii**

1.0 INTRODUCTION **1**

2.0 LITERATURE REVIEW **3**

2.1 Tissue Wound Healing 3
2.2 Transforming Growth Factor-β (TGF-β) 4
2.3 Cellular Contraction 6
2.4 *In Vitro* Models to Study Cellular Contractility 8
2.5 Cellular Contraction versus Collagen Synthesis 11

3.0 SPECIFIC AIMS OF THE THESIS **12**

3.1 Specific Aim 1 13
3.2 Specific Aim 2 14
3.3 Specific Aim 3 15

4.0 HUMAN FIBROBLAST CONTRACTION: AN *IN VITRO* STUDY USING THE TSM AND FPCG MODELS **17**

4.1 Abstract 17
4.2 Introduction 18
4.3 Materials and Methods 20
4.4 Results 22
4.5 Discussion 25

5.0 DEVELOPMENT OF A MULTI-STATION CULTURE FORCE MONITOR SYSTEM **27**

5.1 Abstract 27
5.2 Introduction 28
5.3 Materials and Methods 30
5.3.1 *CFM System* *30*
5.3.2 *Calibration* *33*
5.3.3 *Experiments for Measuring Fibroblast Contraction* *34*
5.4 Results 35
5.5 Discussion 39

6.0 THE DIFFERENTIAL EFFECTS OF TGF-β1 AND TGF-β3 ON HUMAN FIBROLBAST CONTRACTION AND COLLAGEN SYNTHESIS 41

6.1 Abstract 41
6.2 Introduction 42
6.3 Materials and Methods 44
6.3.1 *Cell Culture* *44*
6.3.2 *Measuring Contraction of HPTFs with the FPCG Model* *44*
6.3.3 *Measuring Contraction of HSFs with the CFM System* *45*
6.3.4 *Measurement of Cell Viability* *45*
6.3.5 *Measurement of Collagen Synthesis* *46*
6.4 Results 46
6.5 Discussion 53

7.0 SUMMARY AND FUTURE DIRECTIONS 56

APPENDIX 60

BIBLIOGRAPHY 74

LIST OF FIGURES

Page

Figure 1 HPTFs are contractile, which is demonstrated by the formation of wrinkles (white arrow) underneath the cells (black arrow) plated on a TSM. 22

Figure 2 HPTFs at a high density substantially wrinkle (white arrow) the underlying TSM. Local populations of cells align in a similar direction with the wrinkles forming perpendicular to preferred cell direction. 22

Figure 3 The wrinkles (white arrow) in the TSM are cell-mediated. Addition of trypsin caused the cells to detach from TSM after 30 s (A). The wrinkles disappear after 2h following cell detachment (D). Also notice that wrinkles formed during TSM fabrication (black arrow) are distinguishable from wrinkles produced by cells. 23

Figure 4 HPTFs contract a three-dimensional collagen gel. The area of a cell free collagen gel remains unchanged (A). HPTFs in collagen gel significantly deform the gel to about 25% of its original area, *i.e.* the area of the well, after 48h in 10% FBS (B). 24

Figure 5 FPCG contraction increased with increasing serum concentration. 24

Figure 6 The CFM apparatus in the incubator (**A**) is connected to an external computerized data acquisition unit that displays and records the voltages from the semi-conductor strain gages. The force generated by the CPCG is transmitted to the beam via the wire frames, while the bending of the beam is monitored by the semiconductor strain gages mounted at the base of the beam, near the beam clamp (**B**). 30

Figure 7 Schematic of the gel attachment unit composed of the vyon bar (**A**) to which the FPCG attaches, and the wire frame (**B**) that transmits the force to the beam or fixation unit. 32

Figure 8 Calibration curves for each of the 4 circuits, show the highly linear voltage-force relationships ($R^2 \geq 0.99$). The initial voltage at 0 dynes represents the beams in the horizontal configuration. Although each circuit has a different initial voltage since the Wheatstone bridges were not balanced, the voltages can be "zeroed" during post-processing of the data. 35

Figure 9 A cell free collagen gel in a silicone dish well (30 x 90 mm) remains the size of the well, with no visible deformation (**A**). A FPCG significantly deforms and pulls away from the sides of the dish (white arrow), with the sides of the gel becoming parabolic in shape (**B**). 36

Figure 10 Contraction of HSFs demonstrates the feasibility of the multi-station CFM system to monitor cellular contraction. The cell-free collagen gels maintained a constant force throughout the experiment, whereas the contraction of 2 million HSFs per collagen gel resulted in an average force of 0.2 nN/cell at about 13 hrs. 38

Figure 11 HPTFs (2 million) in a collagen gel produce 20 dynes of maximum contraction force. These tendon fibroblasts have a markedly different contractile pattern and a significantly lower maximum contraction force than HSFs (**Figure 10**). 38

Figure 12 TGF-β3 induces less HPTF contraction of a free-floating FPCG compared to TGF-β1 at 8, 12, 24, and 48 hrs (* $p < 0.05$). 47

Figure 13 Using the CFM system, all dosages of TGF-β1 were found to increase the maximum contraction force of the HSFs in a collagen gel compared to non-treated controls. The 5 ng/mL of TGF-β1 resulted in the largest increase in maximum contraction force (360% of control; black arrow), whereas 1 and 25 ng/mL resulted in similar maximum contraction forces (280% of control). 48

Figure 14 Using the CFM system, it was shown that TGF-β3 affected the initiation of contraction and the maximum force of contraction in a dose dependent manner. Specifically, similar to TGF-β1, 5 ng/mL of TGF-β3 resulted in the earliest contraction and the highest maximum contraction force (180% of control; black arrow). 50

Figure 15 PIP levels (columns) and maximum contraction force (lines) are apparently dosage dependent for both TGF-β1 and TGF-β3. For both isoforms, the 5 ng/mL dose resulted in the largest increase in PIP levels and maximum contraction force. The trend for both collagen synthesis and maximum contraction force are similar for both isoforms, however, TGF-β3 increased PIP levels and maximum contraction force to a lesser degree than TGF-β1. ($n = 1$ for all dosages) 51

Figure 16 Collagen synthesis and cellular contraction have an apparently strong relationship since PIP levels and maximum contraction force appear to have a linear relationship. 53

Figure 17 PGE_2 significantly inhibited HPTF contraction of a collagen gel at 6, 8, 12, and 24h compared with untreated controls and treatment with hydrocortisone (HC). 72

Figure 18 Healing and normal rat MCL fibroblasts have similar initial contraction rates, however, the healing fibroblasts contract with a greater maximum force than the normal fibroblasts. 73

NOMENCLATURE
Acronyms & Symbols

CPCG	Cell Populated Collagen Gel
CFM	Culture Force Monitor
DMEM	Dulbecco's Modified Eagle Medium
FBS	Fetal Bovine Serum
FPCG	Fibroblast Populated Collagen Gel
FF-FPCG	Free-Floating Fibroblast Populated Collagen Gel
HPTFs	Human Patellar Tendon Fibroblasts
HSFs	Human Skin Fibroblasts
MCL	Medial Collateral Ligament
P/S	Penicillin/Streptomycin
PGE_2	Prostaglandin E_2
TGF-β1	Transforming Growth Factor-β1
TGF-β3	Transforming Growth Factor-β3
TSM	Thin Silicone Membrane

1.0 INTRODUCTION

One of the goals in wound healing research is to develop a means to reduce scar tissue formation, thereby improving the quality and function of tissues following injury. Many tissues, including skin and tendons, heal with scar tissue formation [1,2,3,4,5,6,7], which is characterized by varied biochemical composition, distorted tissue architecture, and decreased mechanical properties in comparison with the normal tissue. Unlike adult skin, fetal skin can heal without scar formation [8,9,10,11,12], which results in a tissue that resembles the surrounding tissue in architecture, composition, and function. Although the mechanisms for this healing response remain unclear, fibroblast contraction is thought to play an important role in the different healing responses of adult and fetal tissue [11].

To study cellular contraction, several *in vitro* models, *i.e.* thin silicone membrane (TSM) and cell populated collagen gel (CPCG), have been developed. The TSM model has been used to estimate cellular forces present during cell division[13]. Using the CPCG model, early fetal skin fibroblasts were found to be less contractile than adult skin fibroblasts [12], suggesting that excessive cellular contraction may contribute to formation of scar tissue. In spite of the studies on skin fibroblast contraction, only a few studies have investigated the contractility of tendon fibroblasts [14,15,16]. Additional studies are needed to investigate the potential role of cellular contraction in other cellular responses necessary for wound healing. For example, collagen synthesis is needed for the maintenance and repair of tissues; however, an overproduced

collagen matrix is a characteristic of scar tissue [17]. Further, growth factors, such as TGF-β1 and TGF-β3, have been shown to increase contraction and collagen synthesis of human skin fibroblasts [18], but interestingly, only TGF-β3 reduces the formation of scar tissue in rat skin wounds [17]. Therefore, the overall goal of this thesis project was to enhance tissue healing quality by reducing scar tissue formation. Specifically, we are interested in investigating human fibroblast contractility and the differential effect of TGF-β1 and TGF-β3 on fibroblast contraction and collagen synthesis.

This thesis is organized as follows. Chapter 2 is a brief review of the relevant literature on tissue wound healing, transforming growth factor-β, cellular contraction, *in vitro* models used to study cellular contraction, and the relationship of cellular contraction and collagen synthesis. Chapter 3 presents the specific aims of this thesis. In chapter 4, the TSM and CPCG models were used to determine whether human tendon fibroblasts are contractile. Chapter 5 describes the development of a new multi-station culture force monitor (CFM) system that was then used to quantify and compare contraction of human skin and tendon fibroblasts. Chapter 6 quantifies and compares the effect of TGF-β1 and TGF-β3 on human fibroblast contraction and collagen synthesis. Finally, chapter 7 summarizes the findings of the thesis studies and discusses the implications that these findings have on tissue wound healing in general, and scar tissue in particular. Lastly, the future directions of this project will be discussed.

2.0 LITERATURE REVIEW

2.1 Tissue Wound Healing

The healing response of tissues consists of four phases [4]. The first phase involves an inflammatory response that initiates the healing cascade. The second phase is comprised of restoration of blood supply via angiogenesis to restore blood supply and the beginning of the repair process with migration and proliferation of fibroblasts into the injured site. Wound contraction and synthesis of collagen and proteoglycans are the major events of the third phase. In the fourth phase, the cells remodel the extracellular matrix [4]. Even with this highly orchestrated and intricate wound healing process, many tissues, including skin and tendons, heal with formation of scar tissue [1,2,3,4,5,6,7]. Not only does scar tissue have altered tissue architecture and composition, but in many cases, it may also impede the functions of the healing tissue. For example, a study found that scar tissue significantly decreases the range of motion of the interphalangeal joints after the rupture of a flexor tendon in a rabbit model [19].

Therefore, it is highly desired to reduce the formation of scar tissue, thereby improving the quality and function of tissues following injury. Previous studies have found that fetal skin wounds, unlike adult wounds, can heal without scar formation [9,10,11,20,21,22,23]. It has been proposed that the scar-less formation of skin wounds is an intrinsic property of fetal fibroblasts [11]. For example, an incision into fetal skin implanted subcutaneously in adult athymic mice healed without scar formation, due to the absence of adult fibroblasts. However, incisions to fetal skin implanted cutaneously allowed for the adult fibroblasts to migrate into the wound site, resulting

in formation of scar tissue [11]. Another study found that fetal tendons healed three times faster and without scar formation or loss of function in contrast to similarly injured adult tendons [24]. These findings suggest that if the phenotypic responses of adult fibroblasts can be regulated to simulate those of fetal fibroblasts, then the formation of scar tissue in adults may be significantly reduced and result in near normal tissue function.

2.2 Transforming Growth Factor-β (TGF-β)

One factor that potentially affects the phenotypic differences between fetal and adult tissue healing is the growth factor profile [10,11,21,22,23]. Of particular interest is transforming growth factor-β (TGF-β), which exists as three different isoforms in mammals: TGF-β1, TGF-β2, and TGF-β3 [25]. Since adult tissue, unlike fetal tissue, heals with scar formation [11,26] and TGF-β1 is present in the adult but it is not detected in fetal skin wounds [10,11,21], this suggests that TGF-β1 is one of the major growth factors contributing to the formation of scar tissue in adult skin wounds. In one study, polyvinyl alcohol (PVA) sponges containing 0.01 to 10 ng of TGF-β (the TGF-β isoform used was not specified in this study) were subcutaneously implanted in fetal rabbits. The implants were found to contain an increased number of fibroblasts and inflammatory cells, as well as an increased amount of collagen deposition compared with those treated with the controls, which were PVA sponges with only the TGF-β vehicle [20]. These findings suggest that TGF-β can induce fetal fibroblasts to respond similarly to that of adult fibroblasts and form scar tissue.

In another study, a piece of human fetal skin was implanted subcutaneously into adult nude mice [21]. Interestingly, implantation of 0.01 to 10 μg of TGF-β1 in a cellulose pellet under the fetal skin resulted in formation of scar tissue in amounts proportional to the applied dosage of TGF-β1 [21], providing additional evidence that TGF-β1 is involved in formation of scar tissue. In rabbit flexor tendons, the levels of TGF-β1 and its receptor expression were both elevated in healing tendons compared to normal tendons [27,28], suggesting that the fibroblasts in the healing tendon are most likely stimulated by the elevated levels of TGF-β1.

The effects of all three TGF-β isoforms on skin wounds using Sprague-Dawley rats were investigated in another study [17]. TGF-β1, TGF-β2, TGF-β3, or neutralizing antibodies to the TGF-β isoforms were injected into the wound margins. Injections of either TGF-β1 or TGF-β2 resulted in increased collagen deposition and similar wound architecture compared with controls, which are wounds without the TGF-β injection [17]. Most noteworthy was that injection of TGF-β3 resulted in reduced collagen deposition and a substantial improvement in the wound architecture compared with control wounds [17]. Further, application of neutralizing antibodies to TGF-β1 and TGF-β2 also reduced the formation of scar tissue [17]. These findings indicate that the TGF-β isoforms differentially affect collagen deposition and wound architecture. Therefore, TGF-β1 is again implicated to contribute to formation of scar tissue, whereas TGF-β3 may actually reduce scar tissue. In addition to these findings, another study investigated the effects of a neutralizing antibody to TGF-β1 on the postoperative range of motion at the proximal and distal interphalangeal joints after transection of the flexor tendon in rabbits [19]. This study found that treatment with an antibody to TGF-β1 significantly increased range of motion compared

with the untreated group. Therefore, TGF-β1 may not only impact the biochemical composition and architecture of wounds, but also the function of healing tissues.

These findings suggest that TGF-β1 and TGF-β3 can induce differential responses at the tissue level. Further, at the cellular level, all TGF-β isoforms generally stimulate fibroblast growth [25], and both TGF-β1 and TGF-β3 were found to increase human skin fibroblast DNA synthesis and collagen production [18]. TGF-β is known to be an important growth factor for normal development and repair processes [25]. Since these studies indicate that the TGF-β isoforms may differentially affect tissue healing, particularly the formation of scar tissue, these TGF-β isoforms may also differentially regulate cellular contraction, a necessity for wound closure and healing [26].

2.3 Cellular Contraction

Wound closure is mediated by cellular contraction [26], which is the force a cell exerts on the extracellular matrix. The actin cytoskeleton was found to be a necessary component of cellular contraction [29]. In addition, the interaction between actin and myosin is involved in cellular contraction since myosin light chain kinase inhibitors were found to decrease cellular contraction [30]. Mechanistically, the actin cytoskeleton is attached to the cell membrane integrins and the integrins on the cell surface transmit the forces produced by the actin-myosin interaction to the attached substrate [31]. The cellular contractile forces are proposed to result from the *traction* due to the cell migration and/or the *contraction* of the cells. As discussed in the **Tissue**

Wound Healing section, cells migrate into the injured site [4]. The propulsion of the cell through the matrix is a result of *traction* forces exerted on the matrix by the cells [32,33]. The other source of cellular force results from sedentary cells that *contract*, essentially pulling the matrix in toward the cell [34]. Therefore, forces on the matrix could be a result of a combination of cellular *traction* and *contraction* forces. The studies in this thesis will not distinguish between these two cellular forces; instead, the resultant force of the matrix-cell complex due to the combination of these two forces will be studied.

Most studies on cellular contraction have predominantly focused on skin fibroblasts [12,35,36,37]. Interestingly, fetal skin fibroblasts were found to be less contractile than adult skin fibroblasts *in vitro* [12]. As adult and fetal skin have markedly different healing propensities [11,26], it suggests that fibroblast contraction may contribute to the different healing responses, specifically the formation of scar tissue. In addition to the studies on skin fibroblast contraction, several studies found that calf patellar and rabbit flexor tendon fibroblasts were able to deform fibroblast populated collagen gels (FPCGs) [15,16,38] and that endotenon and synovial fibroblasts exhibit slightly different contractile forces [15,38]. As measure inf a force monitor system, tendon fibroblasts apparently have a different contraction pattern and a significantly lower maximum contraction force over 24h compared to skin fibroblasts [14]. Further, tendon fibroblast contraction can be inhibited by addition of 5-Fluorouracil [38], an antimetabolite, which indicates the ability to regulate tendon fibroblast contraction with exogenous cytokines. These studies on fibroblast contraction provide a basis for investigating fibroblast contractility; however, additional studies are needed to further the understanding of human fibroblast contractility and

the differential effects of TGF-β1 and TGF-β3 on human fibroblast contraction and collagen synthesis.

During tissue wound healing, the ability of cells to contract is important for wound closure [26,39]. However, excessive cellular contraction can result in formation of scar tissue [12,26]. Likewise, if cellular contraction is inhibited, wound healing may be impaired [12,26]. Thus, cellular contraction during wound healing must be in an optimal range to facilitate wound closure and also reduce scar tissue formation.

2.4 *In Vitro* Models to Study Cellular Contractility

Under normal culture conditions, cells plated on polystyrene culture dishes, cellular contractility can not be studied because the substrate that the cells are attached to is too stiff. Since commonly used cell culturing techniques do not allow for visualization or quantification of cellular contraction, *in vitro* models have been developed to study cellular contractility, including the thin silicone membrane (TSM) [13,40] and cell populated collagen gel (CPCG) [12,18,41,42].

A creative solution to the limitation of traditional culture methods was the fabrication of a TSM to which the cells can attach and deform [13,40]. One challenge of this technique is that the membrane must be of very low stiffness so that the small forces produced by the cells can deform the underlying membrane. Fabrication of a TSM is difficult, and the process is further complicated by the need to plate the cells onto the membrane without damaging it. One study

using this model calculated the forces produced by cells during cellular division by measuring the number and length of the wrinkles produced under the cell body [13]. Although this model is capable of demonstrating cellular contractility, several limitations exist. First, the cells are plated on a two-dimensional surface, whereas cells *in vivo* are in a three-dimensional matrix. In addition, the cellular forces can only be qualitatively demonstrated or indirectly estimated based on the extent of wrinkle formation under the cells.

The second model used to study cellular contractility is the CPCG [12,15,16,18,35,37,41,43]. In this model, cells are mixed with a collagen solution and poured into a predefined well. After gel polymerization, the cells are embedded in the collagen gel. To measure the amount of cellular contraction, the area or diameter of the gel is measured. Therefore, a smaller collagen gel area corresponds to a larger cellular contraction force. Further, the rate of contraction is inversely related to collagen concentration and directly dependent on the cell number [36,41,43].

Although measuring the CPCG area can be an efficient and effective means for monitoring cellular contraction, the contraction force is not being measured, *i.e.* the model is a semi-quantitative measurement of cellular contraction. Further, the stiffness of the gel should increase as the gel area becomes smaller, therefore preventing small changes in cellular contraction from being detected. This potentially makes the CPCG model insensitive to distinguish between certain treatments, such as various dosages of a growth factor treatment. Therefore, the CPCG can be a good model for determining if cells are contractile; however, the CPCG model may not be sufficient to quantify and determine small differences between treatments.

To overcome the shortcomings of the TSM and CPCG models, several cell force monitor systems have been developed. The main advantage of these systems is that they can quantify the force of contraction CPCGs [29,36,37,43]. For example, the system developed by Delvoye *et al.* used strain gages to measure forces produced by the FPCGs [36]. The fibroblasts in this system align to the long axis of the FPCG and the force produced by the FPCG is proportional to the number of cells and inversely proportional to the collagen density [36]. In another system, an isometric force transducer was used to measure the FPCG contractile force [29]. The culture force monitor (CFM) system [14,37,43] is a more recent system that quantifies the contractility of CPCGs and can detect different contractile patterns of different cell types [14].

Thus, these CFM systems offer the advantages of quantifying the CPCG contraction and are sensitive enough to determine differences in contraction due to different cell types. In addition, the cells in these systems are in a three-dimensional collagen matrix under tension, which mimics the cells' *in vivo* environment more closely. These systems, however, also have several limitations. Each device can only measure one sample at a time and the conventional strain gages used may not be sensitive enough to detect differences in cellular contraction forces due to minor variations in treatments. Therefore, a more sensitive system that can simultaneously measure forces of multiple CPCGs, while maintaining the three-dimensional matrix is highly desired.

2.5 Cellular Contraction versus Collagen Synthesis

Cellular contraction, being an important component of wound healing, potentially affects other cellular responses necessary for wound healing. During wound repair, the fibroblasts that migrate into the injured site must synthesize collagen to repair the extracellular matrix. Fibroblasts in collagen gels during short term culture (4 days) were found to secrete procollagen into the medium, while during long term culture (4 weeks), the cells synthesized α type I collagen that was incorporated into the matrix [44]. Therefore, the FPCG model can potentially be used to study cellular contraction and collagen synthesis simultaneously. In support of cellular contraction affecting collagen synthesis, the actin cytoskeleton is thought to transduce signals for collagen and procollagenase synthesis, proteins involved in tissue remodeling [45]. Further, in a separate study, disruption of the actin cytoskeleton with cytochalasin D activated procollagenase IV [46]. Since cellular contraction requires the actin cytoskeleton [29], this suggests that cellular contraction may affect other cellular responses, such as collagen metabolism, which are important for wound healing. Therefore, these findings support the project's working hypothesis that regulating cellular contraction may result in a corresponding regulation of other cellular responses, *i.e.* collagen metabolism, which are important for wound healing.

3.0 SPECIFIC AIMS OF THE THESIS

During healing, many types of tissues form scar tissue, which is characterized by an altered biochemical composition, distorted tissue architecture, and decreased mechanical properties [5,6,7,17]. As a result of these altered tissue characteristics, scar tissue can impair the normal function of the tissue. For example, transection of rabbit flexor tendons resulted in formation of scar tissue, which significantly decreased the range of motion compared to those not injured [19]. Regarding the formation of scar tissue, excessive cellular contraction is known to be a contributor [26]; therefore, it is necessary to regulate this cellular response in order to reduce the formation of scar tissue. Recent studies have begun to untangle the intricate mechanisms of wound healing; however, there remains only limited knowledge about the role of cellular contraction during wound healing, particularly in tendons and ligaments. TGF-β1 and TGF-β3, two growth factors predominant in adult tissue healing [47], were both found to increase human skin fibroblast contraction and collagen synthesis [18]. However, TGF-β3 reduced the formation of scar tissue in rat skin wounds compared with TGF-β1 and non-treated controls [17]. It remains to be determined, nevertheless, whether TGF-β1 and TGF-β3 differentially regulate cellular contraction. Therefore, the overall objective of this project is to reduce the formation of scar tissue during healing by regulating cellular contraction. Toward this overall objective, the specific aims of this thesis are to examine human fibroblast contractility *in vitro* and determine the differential effects of TGF-β1 and TGF-β3 on human fibroblast contraction and collagen synthesis, important cellular functions in tissue wound healing.

3.1 Specific Aim 1

To determine whether human tendon fibroblasts are contractile using two *in vitro* models, the thin silicone membrane (TSM) and fibroblast populated collagen gel (FPCG). On one hand, cellular contraction is known to be necessary for wound closure [26]. On the other hand, however, excessive cellular contraction contributes to the formation of scar tissue [12,26]. If tendon fibroblasts are contractile, then regulating the cells' contraction may reduce the formation of scar tissue in tendons.

Hypothesis 1: We hypothesize that human patellar tendon fibroblasts are also contractile, since calf patellar tendon and rabbit flexor tendon fibroblasts have been found to contract collagen gels [14,15,16,38].

3.2 Specific Aim 2

To develop a multi-station culture force monitor (CFM) system to characterize contraction of human fibroblasts in a collagen gel, and use this system to determine whether human tendon and skin fibroblasts exhibit different contraction patterns. Current force monitor systems can quantify FPCG contraction [29,36,37,43]; however, they are limited to testing one sample per device and often require a large number of cells per gel. Using one of these systems, fibroblasts from *rabbit* flexor tendons were found to contract significantly less than *human* skin fibroblasts [14]. The contractility of *human* tendon fibroblasts, however, has yet to be quantified and compared with *human* skin fibroblasts. Different contractile characteristics of cells may provide a basis for the differential healing responses of tissues and indicate the need for tissue specific methods to regulate cellular contraction in order to reduce the formation of scar tissue.

Hypothesis 2: Rabbit flexor tendon fibroblasts were shown to contract significantly less and with a substantially different contraction pattern from human skin fibroblasts [14]. Therefore, we hypothesize that human tendon fibroblasts contract a collagen gel to a lower degree and with a different contraction pattern compared with human skin fibroblasts.

3.3 Specific Aim 3

To determine whether TGF-β1 and TGF-β3 differentially alter human fibroblast contraction and collagen synthesis. It is known that during formation of scar tissue, both cellular contraction and collagen synthesis are over-stimulated [17,26]. Although both TGF- β1 and TGF-β3 were found to increase human skin fibroblast contraction and collagen synthesis, only TGF-β3 was found to reduce the formation of scar tissue in rat skin wounds [17]. Thus, if TGF-β1 and TGF-β3 differentially regulate cellular contraction and collagen synthesis of human fibroblasts, these growth factors may be used to regulate these cellular responses to reduce the formation of scar tissue.

Hypothesis 3: Since TGF-β1 and TGF-β3 elicit different healing responses in rat skin wounds [17], these two isoforms of TGF-β may induce differential effects on the fibroblasts *in vivo*. In order to further understand the actions of these isoforms on human fibroblasts, we tested the hypothesis that treatment with either TGF-β1 or TGF-β3 increases human fibroblast contraction and collagen synthesis in a dose dependent manner compared to non-treated controls. Further, since TGF-β3 reduces the formation of scar tissue, we hypothesize that TGF-β3 increases human fibroblast contraction and collagen synthesis to a lower degree than TGF-β1.

In this thesis, the contractility of human fibroblasts was characterized and the effect of TGF-β1 and TGF-β3 on human fibroblast contraction and collagen synthesis will be determined. The quantitative data obtained from the multi-station CFM system will help to correlate cellular contraction with collagen synthesis, an important cellular response during wound healing. The studies in this thesis also contribute to the understanding of the cellular and molecular mechanisms of tissue wound healing. In addition, by understanding the contraction pattern of cells from a specific tissue, treatments can be tailored to properly regulate the cells' contraction and reduce the formation of scar tissue during healing.

4.0 HUMAN FIBROBLAST CONTRACTION: AN *IN VITRO* STUDY USING THE TSM AND FPCG MODELS

4.1 Abstract

Cellular contraction is necessary for wound closure; however, excessive contraction may lead to the formation of scar tissue. After injury, tendons can heal with scar tissue, characterized by a disorganized collagen matrix and lower mechanical properties compared to normal tendons. Few studies have examined at tendon fibroblast contraction and the role that it may play in tendon healing. Therefore, the objective of this study was to determine whether human tendon fibroblasts contract *in vitro*, using the established TSM and FPCG models. Human patellar tendon fibroblasts (HPTFs) were used in this study and found to significantly deform the TSMs and FPCGs, demonstrating that these cells are contractile. Further, the cells' contraction was dependent on the serum concentration, suggesting that the HPTF contraction can be regulated by environmental factors, such as growth factors. In order to reduce formation of scar tissue, it is important to be able to regulate the cells' contraction. Since cellular contraction is a necessary component of skin healing, these findings suggest that contraction of human tendon fibroblasts may play a role in tendon healing. Thus, additional studies are needed to further characterize human tendon fibroblast contraction and the role that it may play in tendon healing.

4.2 Introduction

Cellular contraction, defined as the force cells exert on the extracellular matrix, plays an important role in tissue wound healing [26]. However, since the cellular forces are very small (~ 1 nN/cell) [29,36,37,43], these forces can not be easily demonstrated, let alone quantified using normal culture techniques, *i.e.* culturing cells on polystyrene culture dishes. An innovative solution to the inability to visualize cellular contraction was developed by Harris *et al.* [40]. Harris and coworkers fabricated a thin silicone membrane (TSM), about 1 μm thick [40]. Using this TSM, cells were cultured and observed with light microscopy. Remarkably, fibroblasts, parenchyma cells, macrophages, and other cells types visibly deformed the TSM, such that wrinkles formed underneath the cell bodies. In a later study using ultraviolet irradiation to fabricate the TSMs consistently, the cellular forces were estimated by measuring the amount of force needed to create the wrinkles seen under the cells [13]. They used calibrated microneedles to "push" the cells, thereby correlating the amount of force with the number and length of wrinkles. Thus, when the cell formed wrinkles in the membrane, they could estimate the amount of force the cell was exerting on the membrane [13].

Another *in vitro* model to study cellular contraction was developed that used a three dimensional collagen gel [41]. In this model, a fibroblast populated collagen gel (FPCG) was formed by the polymerization of a cell-collagen mixture, thereby entrapping the cells in the collagen gel. The area of the FPCG was found to decrease over time. Since cell-free collagen gels did not deform, the deformation was cell-mediated and the cellular contraction could be semi-quantified by measuring the change in FPCG area. Furthermore, this study demonstrated

that the FPCG contraction is inversely dependent on the concentration of collagen and directly dependent on the number of cells [41]. In other words, the more collagen, the stiffer the matrix will be, and the less it will be able to deform. In addition, more cells can generate a larger force, thereby causing greater gel deformation.

Both TSM and FPCG models provide a means to study cellular contraction, but each has its advantages and limitations. The unique advantage of the TSM model is that it allows for visualization and estimation of the forces from a single cell. However, cells are normally in a three-dimensional collagen matrix, such that the FPCG model offers the advantage of a cell being in an environment similar to *in vivo*. Therefore, potential limitations of the TSM model are that it only allows for visualization of a few cells, the cells are on a two-dimensional substrate, and this model is technically demanding, *i.e.* it is difficult to fabricate usable membranes and quantify the cellular forces. The major limitations of the FPCG model include its semi-quantitative measurement of cellular contraction, the inability to quantify the cellular forces of individual cells, and the increase in gel stiffness as a result of the smaller gel area. Overall, however, the FPCG model is advantageous as it provides for a simple, yet effective way to study cellular contraction, as well as simulating the *in vivo* cellular environment.

As there is a great interest in reducing scar tissue formation in dermal wounds, many studies have investigated skin fibroblast contraction [2,12,18,35,48,49,50,51,52,53,54,55,56]. However, only a few studies have investigated tendon fibroblast contractility in collagen gels [14,15,16,38]. Although these studies suggest that tendon fibroblasts contract *in vitro*, cellular contractility is highly dependent on the species and type of cells [14]. These previous studies used calf patellar tendon [16] and rabbit

flexor tendon [14,15,38] fibroblasts; however, studies are needed to determine whether human tendon fibroblasts are also contractile. Therefore, the objective of this study is to test the hypothesis that human tendon fibroblasts contract *in vitro*, using the TSM and FPCG models. Since tendons also heal with scar tissue [5,7,57], understanding human tendon fibroblast contraction may help to reduce the formation of scar tissue in healing tendons.

4.3 Materials and Methods

HPTFs were obtained from pieces of patellar tendon autografts of healthy donors undergoing anterior cruciate ligament reconstruction. The protocol for obtaining the tendon samples was approved by the Institutional Review Board of the University of Pittsburgh Medical Center (Assurance of compliance # IORG0000196). In a laminar flow hood, the tendon samples were washed twice with phosphate-buffered saline (PBS; Invitrogen, CA) and minced in a 100 mm culture dish. The tendon samples were maintained in DMEM supplemented with 10% fetal bovine serum (FBS; Invitrogen) and 1% penicillin/streptomycin (P/S; Invitrogen) in 5% CO_2 at 37^{o}C and 100% humidity. After the HPTFs grew out of the sample and became confluent, the cells were sub-cultured 5 to 7 passages to obtain a sufficient number of cells for experiments.

The protocol for the TSMs was adapted from that described by Harris *et al.* [40]. Briefly, glass microscope coverslips were covered with liquid silicone (RTV ME 601A; Wacker Silicones Corporation, MI). The coated coverslips were inverted and slowly passed over a 1 inch Bunsen burner flame for about 1 second, just long enough to see the surface of the silicone fluid polymerize. The TSMs were then set into a 35 mm tissue culture dish (Falcon) and covered with

a Pronectin-F solution (10 μg/mL) to promote cell attachment. The Pronectin-F solution was washed one time with PBS. To prepare the cells for plating, the HPTFs were trypsinized, centrifuged, and then diluted to various cell densities. The cell solution was pipetted onto the TSM. After 30 minutes of incubation, additional medium was added to cover the TSM. Cells on the TSM were incubated overnight to allow attachment and spreading. Microphotographs were taken using a Nikon inverted microscope (TE200) and camera (Nikon, FX-35DX) for documentation of the wrinkles. In a separate experiment to demonstrate that the TSM wrinkles were cell mediated, HSFs were plated on the TSM. The medium was aspirated and replaced with trypsin to cause the cells to detach from the membrane. Microphotographs were taken at 30s, 30m, 1h, and 2h for documentation

For the FPCGs, a solution of ~98% bovine collagen type I (Cohesion Technologies Inc., CA) was mixed with 0.1 M NaOH and 10X PBS (ratio of 8:1:1). FPCGs were prepared in wells of an untreated 12 well plate (Fisher, PA) by mixing 0.5 mL of the collagen gel solution (2.56 mg/mL) and 150,000 HPTFs in 0.3 mL of AIM-V (Invitrogen), a serum-free medium. After gel polymerization, 1.5 mL of DMEM with 10% FBS and 1% P/S was added to each FPCG. For determining serum dependence, 1.5 mL of DMEM with 0% FBS, 1% FBS, or 10% FBS were added to the corresponding FPCGs. Digital photographs of the gels were taken at 4 time points (12, 24, 36, and 48h) with a Kodak DC3400 camera, and the digital images were analyzed using Scion Image Software (Scion Corporation, Frederick, MD). Gel areas were normalized by the initial area of the gel, *i.e.* the area of the well (3.8 cm^2). Unpaired *t*-test was used for data analysis, with a significance level set at $\alpha = 0.05$.

4.4 Results

HPTFs readily attached and spread on the TSM (**Figure 1**), so that wrinkles (white arrow) formed directly underneath the cells (black arrow), predominantly perpendicular to the long axis of the cell. Further, higher densities of HPTFs resulted in larger numbers of wrinkles throughout the membrane, and localized cells appeared to align in a similar direction and form wrinkles perpendicular to their alignment (**Figure 2**). To demonstrate that the wrinkles on the TSM were cell-mediated, HSFs were plated on a TSM and allowed to attach for several hours. After a 30s incubation with trypsin, the HSFs detached from the TSM (**Figure 3A**). The wrinkles gradually decreased and nearly disappeared after 2 hours (**Figure 3D**). Note that fabrication of the TSMs causes wrinkles (black arrow, **Figure 3A**) that are clearly distinguishable from the wrinkles produced by the cells (white arrow, **Figure 3**).

Figure 1 HPTFs are contractile, which is demonstrated by the formation of wrinkles (white arrow) underneath the cells (black arrow) plated on a TSM.

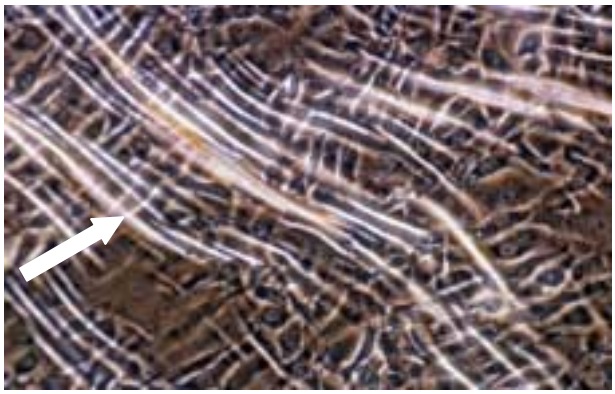

Figure 2 HPTFs at a high density substantially wrinkle (white arrow) the underlying TSM. Local populations of cells align in a similar direction with the wrinkles forming perpendicular to preferred cell direction.

For the FPCG model, the HPTFs were embedded in the collagen gel. Collagen gels without cells underwent no change in area, so the gel remained the size of the well (**Figure 4A**). After a period of 24 hours, the FPCG areas decreased significantly (**Figure 4B**) from the initial area, the area of the well. Moreover, the HPTFs responded differently depending on the concentration of FBS (**Figure 5**). The FPCGs in 10% FBS had a significantly smaller gel area compared with those in 1% FBS. The HPTFs in 0% FBS were rounded in shape and not well integrated into the collagen gel, with no detectable change in gel area.

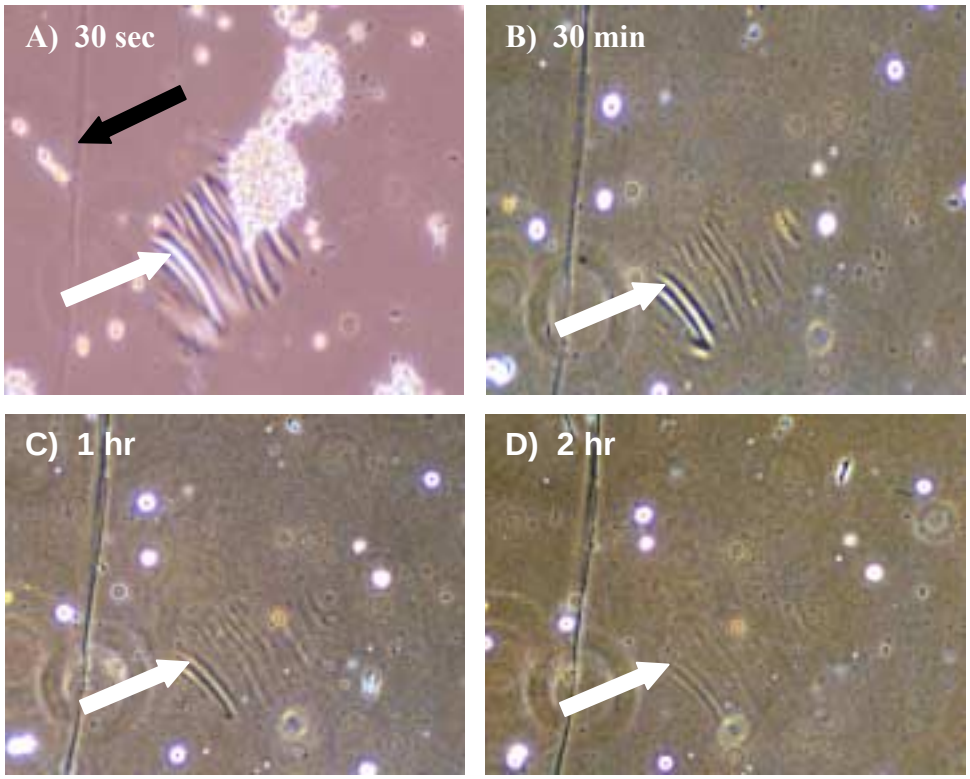

Figure 3 The wrinkles (white arrow) in the TSM are cell-mediated. Addition of trypsin caused the cells to detach from TSM after 30 s (A). The wrinkles disappear after 2h following cell detachment (D). Also notice that wrinkles formed during TSM fabrication (black arrow) are distinguishable from wrinkles produced by cells.

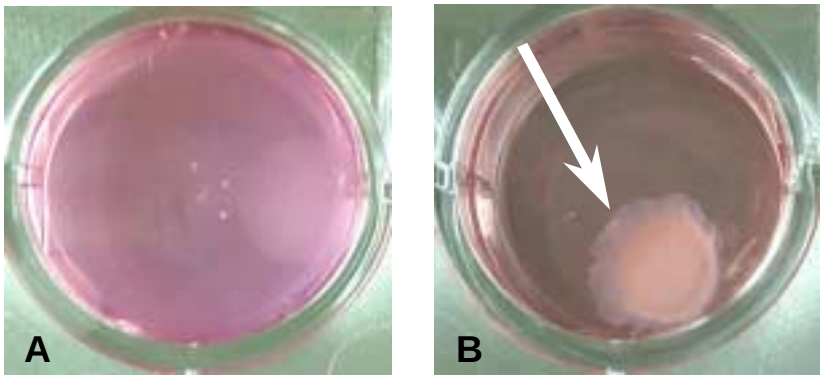

Figure 4 HPTFs contract a three-dimensional collagen gel. The area of a cell free collagen gel remains unchanged (A). HPTFs in collagen gel significantly deform the gel to about 25% of its original area, *i.e.* the area of the well, after 48h in 10% FBS (B).

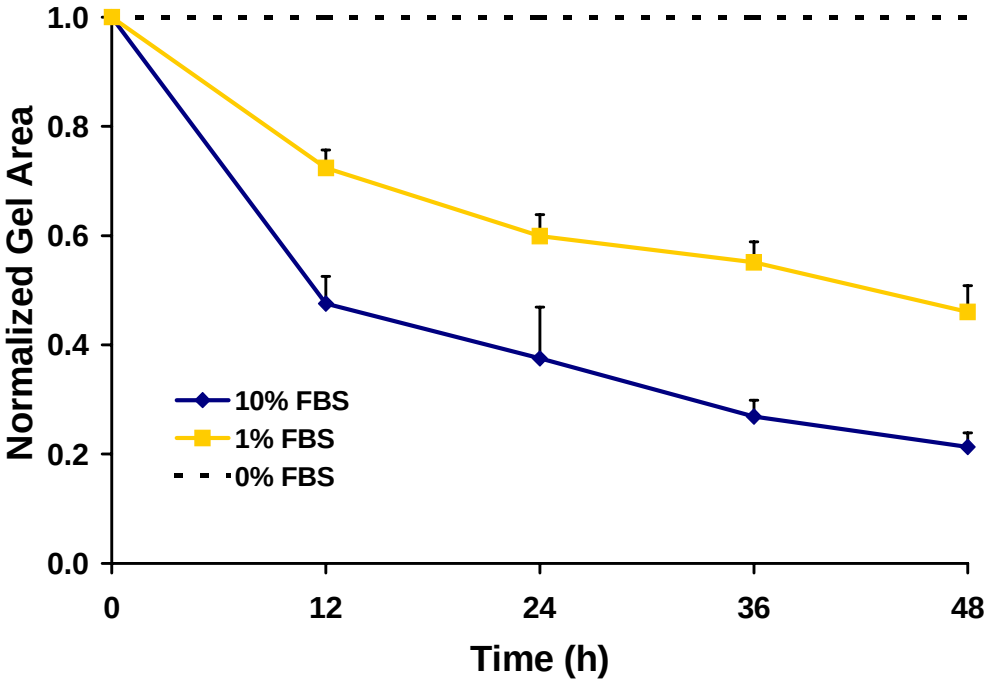

Figure 5 FPCG contraction increased with increasing serum concentration.

4.5 Discussion

In this study, HPTFs were found to deform both TSMs and collagen gels, indicating that these human tendon fibroblasts are contractile. In addition, the FPCG contraction was found to be dependent on serum concentration. Since cellular contractility is necessary for wound closure [26], these findings suggest that tendon fibroblast contractility can be further studied to understand its role in tendon healing. The finding that HPTF contraction depends on the concentration of FBS demonstrates the ability of biological factors to regulate HPTF contraction.

Although both the TSM and FPCG models were used to demonstrate HPTF contraction, the magnitude of the contraction force has yet to be determined. Further, a method to consistently plate the cells on the TSM without damaging the membrane proved to be difficult. Often, the membrane would break and the liquid silicone underneath the membrane would leak out, thereby increasing the friction between the TSM and coverslip. Thus, the cellular forces were not able to overcome the frictional force, therefore preventing the formation of the wrinkles. The FPCG model, although a semi-quantitative way to measure cellular contraction, was considerably easier to use than the TSM and appears to be a useful method for investigating cellular contraction. An apparent limitation of the FPCG model is that as the collagen gel contracts, the gel should become denser, therefore increasing its stiffness. This may limit the sensitivity of the model because as the gel increases in stiffness, a larger force is needed to deform the gel. Therefore, treatments causing only small changes in cellular contraction may not be distinguishable because the differences in cellular forces may not cause detectable changes in gel areas.

This study demonstrates that human tendon fibroblasts are contractile. The TSM model qualitatively demonstrated HPTF contraction, whereas the FPCG model semi-quantitatively measured the cells' contraction. Addressing the shortcomings of the FPCG model, several force system have been developed [29,36,37,43]. With further studies on tendon fibroblast contraction, means to regulate the cells' contraction may be investigated to potentially reduce the formation of scar tissue in healing tendons. For future studies, a force system will be developed to monitor contraction of multiple FPCGs simultaneously, allowing human fibroblast contractility to be quantified for comparison between cells from different tissues and cells exposed to growth factors, *i.e.* TGF-β1 and TGF-β3.

5.0 DEVELOPMENT OF A MULTI-STATION CULTURE FORCE MONITOR SYSTEM

5.1 Abstract

Cellular contraction contributes to the formation of scar tissue. To study the contractility of cells *in vitro* and its potential contribution to scar tissue formation, a multi-station culture force monitor (CFM) system has been developed. This system consists of four vertical cantilever beams with semiconductor strain gages and a computerized data acquisition unit to monitor contractile forces of the cells in a collagen gel. Calibration showed that this system has a highly linear voltage-force relationship ($R^2 > 0.99$). Using this system, we tested the hypothesis that human patellar tendon fibroblasts (HPTFs) and human skin fibroblasts (HSFs) exhibit different contraction patterns and maximum contraction force. The HPTFs (0.1 nN/cell) were found to contract with about half of the maximum contraction force produced by the HSFs (0.2 nN/cell). These findings are consistent with the range found in literature. The unique features of this system are the use of semi-conductor strain gages to increase sensitivity and the ability to simultaneously test multiple samples. Further, using this system, fibroblasts from different tissues were differentiated based on their contractile patterns, suggesting that treatments to regulate cellular contraction need to be tailored to the specific tissue. Future studies will investigate treatments that have the potential to regulate cellular contraction and reduce the formation of scar tissue.

5.2 Introduction

Thus far, human skin and tendon fibroblasts were shown to be contractile using the thin silicone membrane (TSM) and cell populated collagen gel (CPCG) models (**Chapter 4**). However, both of these models have certain limitations for studying cellular contractility. The TSM uses a two-dimensional membrane, is primarily qualitative, and is difficult to use for experiments. The CPCG model has several advantages compared with the TSM model; it is a three-dimensional matrix similar to *in vivo* and it is relatively simple to use. However, the main limitations of the CPCG model are that it may be insensitive to slight differences in experimental conditions and it is semi-quantitative. Therefore, it is highly desired to use a system that can quantify cellular contraction forces. Several force systems have been developed to address these limitations [29,36,37,43]. Systems using strain gages were developed to measure forces of FPCGs [36,37]. They showed that the fibroblasts in this system align to the long axis of the FPCG and skin fibroblasts produced 0.1 to 1 nN/cell [36,37]. Further, the cell-mediated contraction force was found to be proportional to the number of cells and inversely proportional to the collagen density [36]. Another system used an isometric force transducer to measure the FPCG contractile force [29] and found human skin fibroblasts to produce about 0.6 nN/cell on average. These studies clearly illustrate the difficulty in measuring cellular contraction, as the contraction force is on the order of 1 nN/cell. Therefore, many of these systems use 5 to 10 million cells per collagen gel so the resultant force is large enough to detect.

The most recent force system used to measure cellular contraction is the culture force monitor (CFM). It can measure FPCG contraction like the other systems, but with better

resolution, and therefore it only needs to use 2 to 5 million cells per gel [37,43]. For the CFM, the CPCG is formed in a silicone well with two porous polymer bars on the sides or ends of the well, such that when the gel polymerizes, it is attached to the polymer bars. A wire frame extends from the polymer bars, such that one end of the gel is connected to a cantilever beam with strain gages attached at its base, while the other end is held fixed. Thus, the force produced by the CPCG is transferred via the wire frame to the beam, causing the beam to bend. The strain gages at the base of the beam monitor the resultant strain due to beam bending. By calibrating the beam with known weights, the force produced by the CPCG can be calculated directly from the voltage recorded by the strain gages.

These systems are quite sensitive, measuring CPCG contraction in the range of 1200 dynes (1 dyne = 10^{-5} N) for about 10 million cells, corresponding to about 1.2 nN/cell [43]. Because of the need to compare the effect of biological factors (e.g., growth factors) that play an important role in wound healing, as well as study the effect of cellular contraction on collagen synthesis, a multi-station culture force monitor (CFM) system has been developed. This multi-station CFM system facilitates statistical design and analysis of experiments to study cellular contractilityby testing four samples simultaneously under similar environment conditions. Thus, this chapter presents the design and development of this new multi-station CFM system. Human skin fibroblasts were chosen to demonstrate the feasibility of this system as they are easy to culture, abundant, and their contractile forces are well documented in literature [14,29,36,37,43]. Further, the contractile patterns and maximum contraction force of HSFs and HPTFs in a collagen gel will be compared using the data obtained from this new CFM system.

5.3 Materials and Methods

5.3.1 CFM System

The new multi-station CFM system consists of the CFM apparatus (**Figure 6A**) and a computerized data acquisition unit, capable of simultaneously monitoring contractile forces of multiple CPCGs. The base of the CFM apparatus is an aluminum platform that can accommodate up to six circuits, each capable of monitoring CPCG contraction. The support rod assembly mounted to the base of the CFM provides a framework for positioning and fixing the beam-clamps (**Figure 6B**). Further, the fixation units opposing the support rod assembly allow one end of the gel to be fixed, as well as providing a means for adjusting gel tension. The beam clamps, made of stainless steel, rigidly fix the beams and can move along the support rod assembly for proper positioning during experiments.

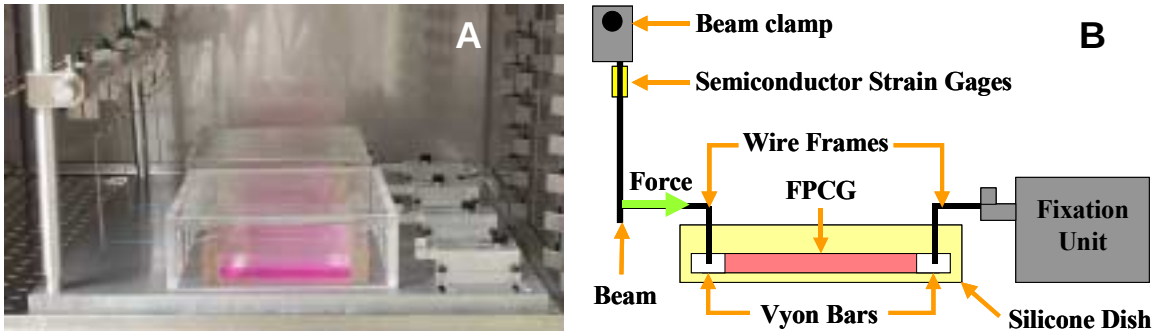

Figure 6 The CFM apparatus in the incubator (**A**) is connected to an external computerized data acquisition unit that displays and records the voltages from the semi-conductor strain gages. The force generated by the CPCG is transmitted to the beam via the wire frames, while the bending of the beam is monitored by the semiconductor strain gages mounted at the base of the beam, near the beam clamp (**B**).

The beams, which detect the cellular contractile forces, are made of aluminum (95.2 x 5.0 x 0.25 mm; Young's modulus, E = 70 GPa), permitting sufficient beam strain under the expected CPCG forces in our CFM system (~ 200 dynes). A small suture loop (braided polyester suture, 4-0; Ethicon, NJ) tied to the beam through a 0.4 mm hole located 76.2 mm from the clamp connects the gel attachment unit to the beam. To measure beam strain, two semiconductor strain gages were mounted on each side of the beam (gage factor = 140; resistance ~ 400Ω; Micron Instruments, CA) in a full Wheatstone bridge configuration, located 1.6 mm from the clamp. In addition, a power supply (Hewlett Packard 6237B Power Supply) provides 4V DC excitation voltage to all the semiconductor strain gages.

The silicone dishes (70 x 30 x 10 mm) that contain the CPCGs, are custom made using a molding process as described previously [58]. Briefly, two silicone components (RTV ME 601A and 601B; Wacker Silicones Corporation, MI) are mixed in a ratio of 10:1. After being degassed, the silicone mixture is poured into a multiple-dish mold made of acrylic (Plexiglass). The silicone dishes obtained from this molding process are hydrophobic, thereby minimizing the attachment of cells and the collagen gel to the dish. Each silicone dish contains three separate wells, and the dish height was decreased to accommodate the connection of the CPCGs to the beams and fixation units.

The force generated by the cells is transmitted from the CPCG to the beam via the gel attachment unit (**Figure 6B**). The gel attachment unit (**Figure 7**) is composed of two parts, a porous vyon bar and a wire frame. The CPCGs polymerize into the porous vyon bars (23 x 8 x 3 mm; Porvair Inc., NC) located at the ends of the silicone dish. The wire frames (0.36 mm

stainless steel wire) extend vertically from the vyon bars to allow easy attachment to the beam and tension unit. As one end of the gel is fixed by the tension unit, the contraction of the CPCG is transmitted to the beam by the gel attachment unit and suture, causing the beam to deflect, which is monitored by the semiconductor strain gages (**Figure 6B**).

The data acquisition unit that receives the signal voltage is composed of a data acquisition (DAQ) card (6024E; National Instruments, TX), shielded connector block and cable (National Instruments, TX), and a personal computer. A Labview 5.1 program was developed to display and record the output voltage signals from the semiconductor strain gages (see description in **Appendix**). The Labview program can record signals at various time points and variable sampling rates. For experiments in this study, the voltage signals were recorded for 10 seconds at 10 Hz, every 10 minutes. Each data point corresponds to the mean of the respective 100 samples.

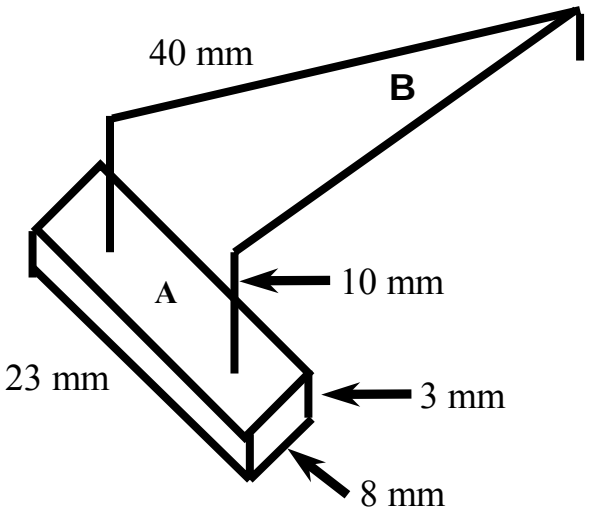

Figure 7 Schematic of the gel attachment unit composed of the vyon bar (**A**) to which the FPCG attaches, and the wire frame (**B**) that transmits the force to the beam or fixation unit.

5.3.2 Calibration

Calibration was performed for each individual circuit, *i.e.*, the components required to monitor each individual beam deflection (beam, strain gages, wire, connecting block, computer, and Labview program). For calibration, the beams were set in a horizontal position, such that known weights could easily be suspended from the beam via the suture loops. The force from the weight causes the beam to bend, and the resulting beam strain is detected by the strain gages. Force is related to strain as shown by the following equation: $P = E*b*\varepsilon*h^2/(6*L)$; P is a point force, E is Young's modulus, b is the beam width, ε is the beam strain, h is the beam thickness, and L is the distance from the location of the point force to the location of the strain gages. Wires of different lengths were cut and weighed using an analytical balance (accuracy of about 1.6 dynes; A-200D, Denver Instrument Company, CO). The weights of six wire pieces were 20, 39, 58, 77, 120, and 243 dynes, which covered the expected range of cellular contractile forces for about two million cells. For each applied weight, 300 voltage outputs (10 Hz for 30s) were recorded and averaged to obtain one data point. This calibration was repeated three times. Linear regression yielded the voltage-force relationship for each circuit. Therefore, the calibration factor for each circuit, which is the slope from the linear regression of the voltage and force data, is used to calculate the force for a given voltage. Note that the calibration was performed in the same environment as that for monitoring cellular contractile forces, in an incubator at 37^oC, 5% CO_2, and 100% humidity. After about three months, the CFM system was recalibrated. Although there was a change in the baseline voltages, the calibration factors remained similar to the previous calibration.

5.3.3 Experiments for Measuring Fibroblast Contraction

HSFs and HPTFs were maintained in DMEM supplemented with 10% fetal bovine serum (FBS) and 1% penicillin/streptomycin (P/S; Invitrogen, CA) in 5% CO_2 at 37^{o}C and 100% humidity. The cells were sub-cultured to obtain sufficient numbers of cells for each experiment (HSFs – passage < 20; HPTFs – passage < 8). A collagen gel solution was made by mixing collagen stock solution (~98% bovine collagen type I; Cohesion Technologies Inc., CA), 0.1 M NaOH, and 10X PBS in a ratio of 8:1:1. FPCGs were prepared in the rectangular silicone dishes by mixing 5 mL of the collagen gel solution (2.56 mg/mL) and $2x10^6$ HSFs or HPTFs in 3 mL of medium. The FPCG solution was pipetted into the silicone dish and around the porous vyon bars. The FPCGs were incubated for 10 minutes to initiate gel polymerization, which was followed by the addition of 7 mL of medium to each dish to allow FPCG to float in the medium. For all experiments in this study, DMEM supplemented with 10% FBS and 1% P/S was used. The FPCGs were attached to the multi-station CFM system and a pretension of 2 to 5 mV, or 4 to 10 dynes, was applied to each FPCG. The FPCG forces were monitored for about 20h. Since HSFs reach a maximum level of contraction after about 8h and gradually decreasing after about 13h, monitoring cellular contraction for 20h allows the rate of initial contraction and the maximum contraction force to be determined. Voltage readings taken every 10 minutes at 10 Hz for 10 seconds were averaged to yield one data point, resulting in 6 data points/h. To demonstrate that the FPCG forces were dependent on cell number, FPCGs were formed with 0, 2, and 3 x 10^6 HSFs/gel and their contraction was monitored for 20h.

5.4 Results

A CFM system with four circuits was successfully developed to measure cellular contractile forces (**Figure 6A**). The weight calibration of the system was effective and repeatable. With this method of calibration, it was shown that there was a highly linear voltage-force relationship for all four circuits ($R^2 > 0.99$) (**Figure 8**). This linear relationship means that the voltage output from the semiconductor strain gages is proportional to the force bending the beam throughout the range of the forces tested (≤ 240 dynes). Thus, the calibration factors, *i.e.*, the slopes of the voltage-force lines from linear regression, for the four circuits were found to be

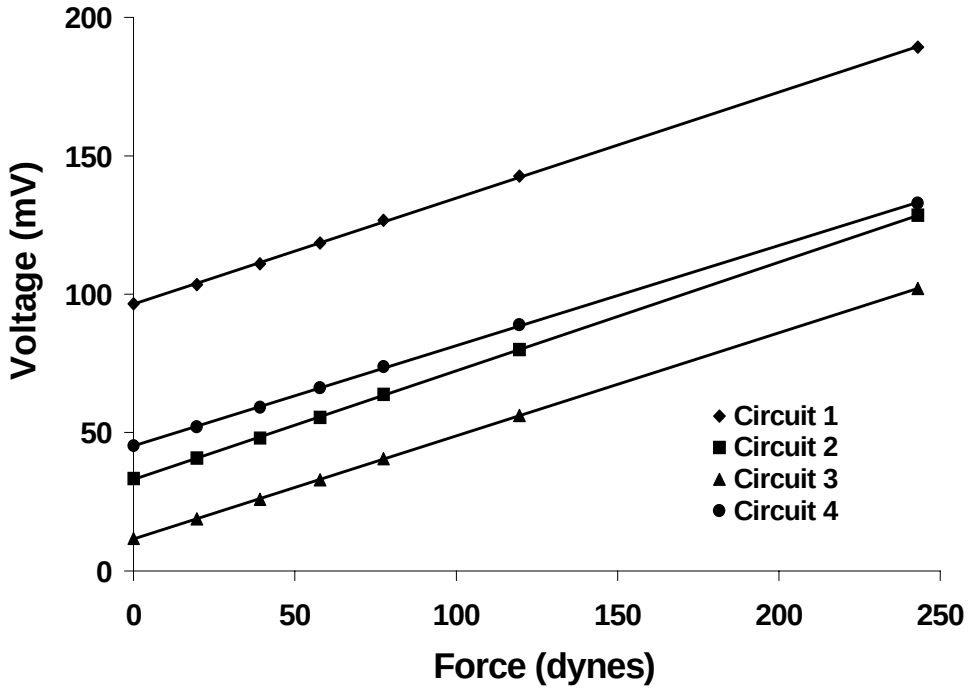

Figure 8 Calibration curves for each of the 4 circuits, show the highly linear voltage-force relationships ($R^2 \geq 0.99$). The initial voltage at 0 dynes represents the beams in the horizontal configuration. Although each circuit has a different initial voltage since the Wheatstone bridges were not balanced, the voltages can be "zeroed" during post-processing of the data.

2.6, 2.6, 2.7, and 2.8 dynes/mV. Repeated calibration after several months resulted in nearly the same calibration factors, with only a shift in the baseline voltage for each circuit. Further, the accuracy of the CFM system on average was determined to be about 1 dyne.

To demonstrate the feasibility of this CFM system, contractile forces of HSFs in a collagen gel were measured. Visually, the cell-free collagen gel remained the same area of the silicone dish (**Figure 9A**), whereas the sides of the FPCG deformed into a parabolic shape (**Figure 9B**), indicating that the HSFs are contractile. Further, force measurement with the CFM system showed that the cell-free collagen gels produced forces less than 10 dynes (**Figure 10**). In contrast, 2 x 10^6 HSFs in a collagen gel produced a maximum force of about 45 dynes, corresponding to ~ 0.2 nN/cell on average (**Figure 10**). The contraction pattern of these HSFs can be divided into four different phases, phase I through phase IV. The first phase begins after the FPCGs are attached to the CFM and ends at the time that

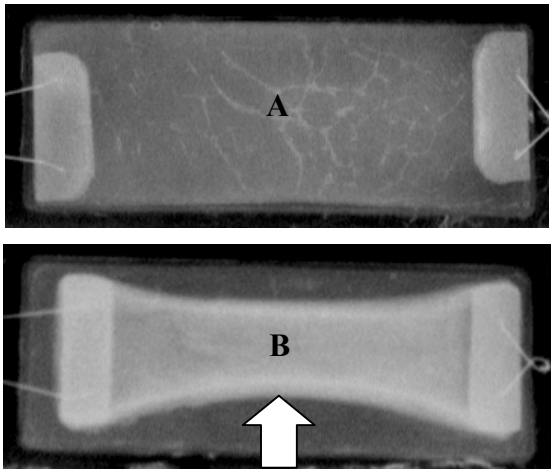

Figure 9 A cell free collagen gel in a silicone dish well (30 x 90 mm) remains the size of the well, with no visible deformation (**A**). A FPCG significantly deforms and pulls away from the sides of the dish (white arrow), with the sides of the gel becoming parabolic in shape (**B**).

the contraction curve reaches the minimum force value (0 to 2h). During the second phase, which consists of the initial increase in contraction force (3 to 7h), the FPCG force rapidly increased to ~ 45 dynes, the maximum force produced by the FPCG. During phase III, the force reaches an equilibrium force, followed by a slow decrease in force during the fourth phase. Notice that the similar contractile patterns of the two FPCGs (**Figure 10**) are due to the same experimental conditions applied.

Further, the HPTFs (2 million) in a collagen gel produced a significantly different contractile pattern (**Figure 11**) than HSFs (2 million; **Figure 10**). The contraction force of the HPTFs increased throughout the experiment. The contraction force reached a temporary equilibrium force from 5 to 10h, followed by a second and greater rise in force. The force rate then decreased, approaching an apparent equilibrium level after 20h. The maximum of about 20 dynes for 2 million HPTFs was recorded at the end of the experiment (~ 36h), corresponding to 0.1 nN/cell on average, which is half of the maximum force produced by the HSFs. Notice again, the similar contractile patterns between these two FPCGs in this experiment under the same experimental conditions (**Figure 11**), indicating that the results from the different circuits are reliable and comparable. In all experiments, cell viability was measured using an MTT assay to verify that the cells were viable.

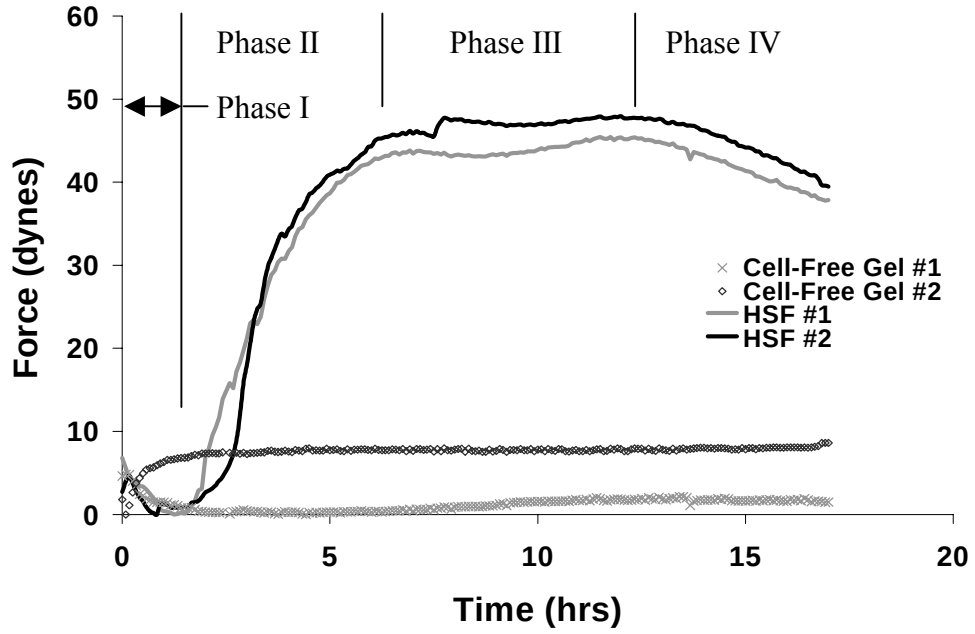

Figure 10 Contraction of HSFs demonstrates the feasibility of the multi-station CFM system to monitor cellular contraction. The cell-free collagen gels maintained a constant force throughout the experiment, whereas the contraction of 2 million HSFs per collagen gel resulted in an average force of 0.2 nN/cell at about 13 hrs.

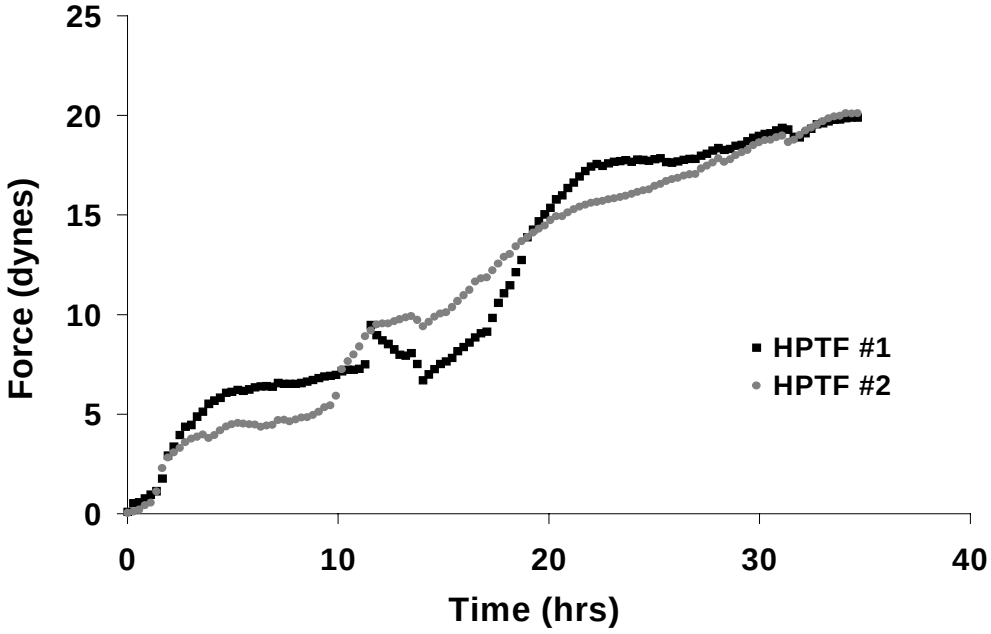

Figure 11 HPTFs (2 million) in a collagen gel produce 20 dynes of maximum contraction force. These tendon fibroblasts have a markedly different contractile pattern and a significantly lower maximum contraction force than HSFs (**Figure 10**).

5.5 Discussion

In this study, a multi-station CFM system was successfully developed to investigate cellular contractility. Calibration of the system demonstrated a highly linear relationship ($R^2 > 0.99$) between the voltage output and applied force. The most significant advantage of this system, however, is its ability to test multiple samples simultaneously. This feature facilitates statistical design and analysis of experiments to study the effects of growth factors, such as TGF-β [18], on cellular contractility.

To demonstrate the feasibility of this system in measuring cellular contraction, HSFs were used because they are readily available, easy to culture, and most importantly, their contractility is well documented [14,29,37,43]. Using this system, HSFs were found to produce 0.2 nN/cell on average. This result is consistent with previous studies using similar devices, which showed that skin fibroblasts in a collagen gel produce between 0.1 and 10 nN/cell [29,36,37,43]. Similar to previous systems, this CFM system only measures contraction of a population of cells in a collagen matrix, not of the individual cells. Therefore, the value of force/cell is a calculated average force that can only be considered as a rough estimate for comparison with previous studies. The resultant contraction pattern (shape, contraction rate, initial contraction time) and the maximum FPCG force are better characteristics for comparison.

Due to the nature of this system, setup of the FPCG, particularly the connection of the FPCG to the CFM system is necessary for obtaining data. A potential problem with this system is that the FPCG can stick to the sides of the silicone dish, preventing force to be transferred to

the CFM system. To minimize the occurrence of this problem, the vyon bars are placed a small distance from the end of the well to minimize their interaction with the silicone dish, and the silicone dishes are replaced as necessary, as the problem of FPCG attachment to the dish is more apparent in the older silicone dishes. More noteworthy are the main advantages of this system over the previous force systems: 1. Because of the increases sensitivity due to the semiconductor strain gages, only 2 million cells/gel are needed to detect contractile forces for the fibroblasts tested; 2. Four FPCGs can be tested simultaneously in the same system, minimizing the variability due to time and environments; 3. The contraction patterns between the beams are surprisingly similar, allowing for comparison of contraction patterns between the beams.

Using this multi-station CFM system, this study showed that contractile patterns and the maximum contraction force are strikingly similar under the same experimental conditions, indicating that this system is reliable and can be used to compare cellular contraction patterns under different treatments. Further, this study demonstrated that HSFs have a significantly different contractile pattern and maximum contraction force compared to HPTFs, suggesting that this system can be used to differentiate between cells from different sources. Thus, this new multi-station CFM system will be a useful tool to study the effects of biological factors (*e.g.* growth factors) on cellular contraction. In addition, this system can be used to examine the effects of cellular contraction on collagen production, which is known to be involved in the formation of scar tissue.

6.0 THE DIFFERENTIAL EFFECTS OF TGF-b1 AND TGF-b3 ON HUMAN FIBROBLAST CONTRACTION AND COLLAGEN SYNTHESIS

6.1 Abstract

Transforming growth factor-β1 (TGF-β1) and TGF-β3, which play important roles in the maintenance and repair of tissues, were both found to increase cellular contraction *in vitro*, but only TGF-β3 was found to reduce the formation of scar tissue *in vivo*. Since excessive cellular contraction can contribute to formation of scar tissue, an overproduced disorganized collagen matrix, we hypothesize that TGF-β3 increases human fibroblast contraction and collagen synthesis to a lesser degree than TGF-β1. To test this hypothesis, the multi-station culture force monitor system was used to measure the contractility of FPCGs. Both, the contraction pattern and collagen synthesis were found to be TGF-β1 and TGF-β3 dose dependent. The 5 ng/mL dose of TGF-β1 or TGF-β3 resulted in the largest increase in maximum contraction force (360% and 180% of controls, respectively) and procollagen levels (750 and 600 ng/mL, respectively) compared to the other dosages (1 and 25 ng/mL). Further, TGF-β3 induced less cellular contraction and collagen synthesis than TGF-β1 at each dosage. Also, the preliminary data suggested that a strong correlation existed between the maximum contraction force and degree of collagen synthesis. These findings suggest that TGF-β3 may induce a lesser degree of cellular contraction and collagen synthesis in healing tissues compared to TGF-β1.

6.2 Introduction

Growth factors are known to play an important role in the maintenance and repair of tissues. Of interest in this study are two transforming growth factor-β (TGF-β) isoforms: TGF-β1 and TGF-β3. As noted previously, unlike adult skin wounds, fetal skin wounds heal without scar formation [20,26]. Further, all the TGF-β isoforms were found to be up-regulated in adult wounds, but remained unchanged in fetal wounds [47], suggesting that these growth factors may contribute to the different healing responses in adult and fetal tissues. More importantly, the higher level of TGF-β3 compared to that of TGF-β1 is important in regulating the healing process in fetal tissue and may contribute to the scar-free healing [59]. In an earlier study, these two TGF-β isoforms were found to have differential effects on the formation of scar tissue: TGF-β3 reduced the formation of scar tissue, whereas TGF-β1 induced the formation of scar tissue in rat skin wounds compared to the non-treated controls [17]. In another study, a neutralizing antibody to TGF-β1 increased postoperative range of motion at the proximal and distal interphalangeal joints after transection of the flexor tendon in rabbits [19], implying that TGF-β1 is involved in formation of scar tissue, and down-regulation of TGF-β1 levels can limit adhesion and scar formation, and thus improve tendon function.

At the cellular level, TGF-β1 and TGF-β3 have both been found to regulate cellular processes important for tissue wound healing, namely increasing skin fibroblast contraction, proliferation, and collagen synthesis [12,18]. However, as a differential response is seen by the

application of either TGF-β1 or TGF-β3 to healing tissues, one would expect a corresponding differential response at the cellular level, *i.e.* cellular contraction and collagen synthesis.

Cellular contraction, the force cells exert on the extracellular matrix, is a necessary component for wound contraction [26]. In spite of its necessity, excessive cellular contraction contributes to the formation of scar tissue [12,26]. A previous study has shown that TGF-β1 and TGF-β3 increase human skin fibroblast contraction [18]. However, since that study was unable to detect differences in cellular contraction from the TGF-β1 and TGF-β3 treatments, further studies are needed to determine if these growth factors induce differences in cellular contraction. Although most studies on cellular contraction investigate skin fibroblasts, recent studies found that tendon fibroblasts are also contractile [14,15,16], which may affect tendon healing. As cells have inherently different contraction patterns and responses to growth factors, studies are also needed to determine if TGF-β1 and TGF-β3 have similar effects on fibroblasts from a different tissue, *i.e.* tendon.

Therefore, the objective of this study was two-fold. The first was to determine whether TGF-β1 and TGF-β3 increase contraction of fibroblasts derived from human tendon and skin in a dose dependent manner; and the second was to determine if TGF-β1 treatment increases human skin fibroblast contraction and collagen synthesis to a greater degree than TGF-β3. For the first objective, HSFs and HPTFs were used. For the second objective, HSFs were chosen because their contractility and the effects of TGF-ß1 and TGF-ß3 are well documented [14,18,29,37,43,60]

6.3 Materials and Methods

6.3.1 Cell Culture

Pieces of patellar tendon autografts were obtained from healthy donors undergoing anterior cruciate ligament reconstruction. The protocol for obtaining the tendon samples was approved by the Institutional Review Board of the University of Pittsburgh Medical Center (Assurance of compliance # IORG0000196). These tendon samples were used for explant cultures to obtain the human patellar tendon fibroblasts needed for the experiments. Briefly, the tendon samples were washed twice with phosphate-buffered saline (PBS; Invitrogen, CA) and minced in a 100 mm petri dish in a laminar flow hood. The HPTFs were maintained in DMEM supplemented with 10% fetal bovine serum (FBS; Invitrogen) and 1% penicillin/streptomycin (P/S; Invitrogen) and in an atmosphere of 5% CO_2 at 37^{o}C and 100% humidity. The HPTFs were left to grow out of the tendon sample, with the medium replaced every 3 days. To obtain sufficient numbers of cells for experiments, the cells were sub-cultured 5 to 7 passages. HSFs (passage < 20) were also maintained in DMEM supplemented with 10% FBS and 1% P/S.

6.3.2 Measuring Contraction of HPTFs with the FPCG Model

For the FPCGs, a solution of ~98% bovine collagen type I (Cohesion Technologies Inc., CA) was mixed with 0.1 M NaOH and 10X PBS (ratio of 8:1:1). Free-floating FPCGs were prepared in wells of an untreated 12 well plate (Fisher, PA) by mixing 0.5 mL of the collagen gel solution (2.56 mg/mL) and 150,000 HPTFs in 0.3 mL of AIM-V (Invitrogen), a serum free medium. After gel polymerization, 1.5 mL of AIM-V medium containing TGF-β1 (1, 5, and 25 ng/mL), TGF-β3 (1, 5, and 25 ng/mL), or no TGF-β for controls was added to each well.

Dosages were chosen based on those used in literature [18]. For the experiment, each dosage was applied to three FPCGs. Photographs of the gels were taken at 5 time points (4, 8, 12, 24, and 48 h) with a digital camera (Kodak DC 3400). The digital images were analyzed using Scion Image Software (Scion Corporation, Frederick, MD), and the resulting gel areas were normalized by the initial area of the gel, *i.e.* the area of the well (3.8 cm^2). Unpaired *t*-test was used for statistical analysis of the data, with a significance level set at $\alpha = 0.05$.

6.3.3 Measuring Contraction of HSFs with the CFM System

FPCGs used in the CFM system (**Chapter 5**) were prepared in rectangular silicone dishes by mixing 5 mL of the collagen gel solution and $2x10^6$ HPTF in 3 mL of AIM-V, a serum-free medium. The FPCG solution was pipetted into the silicone dish and around the vyon bars. The FPCGs were incubated for 10 minutes, followed by addition of 7 mL of AIM-V to each dish with the appropriate treatments. For each experiment, four samples were tested simultaneously, *e.g.*, 1) FPCG without TGF-β; 2) FPCG with 1 ng/mL TGF-β; 3) FPCG with 5 ng/mL TGF-β, and 4) FPCG with 25 ng/mL TGF-β. These dosages were based on those used with the free-floating FPCG model. The FPCGs were attached to the multi-station CFM system and contraction was monitored for 48h. For all experiments, voltage signals were recorded for 10 seconds at 10 Hz every 10 minutes. Each data point corresponds to the mean of the 100 voltage samples recorded every 10 minutes.

6.3.4 Measurement of Cell Viability

To determine the viability of the human fibroblasts at the end of the experiment, an MTT assay was used [61]. Briefly, 200 μL (or 500 μL for CFM) of MTT solution (5 ng/mL) was added

to the medium of the FPCGs. These were then incubated at 37°C and 5% CO_2 for 3h. The supernatant was aspirated, and 2 mL (or 4 mL for CFM) of extraction buffer (15 mL DMF, 14.1 ml H_2O, and 6 g SDS) was added to each dish. After overnight incubation at 37°C, the solution was diluted 1:5 with DI H_2O and mixed thoroughly. Duplicate samples of 200 μL were aliquotted into a 96-well plate, and the absorbance, or optical density (OD) value, was measured using a microplate reader (Spectra MAX 190, Molecular Devices, CA) at 550 nm. The resultant OD value represents the number of viable cells in each sample.

6.3.5 Measurement of Collagen Synthesis

Collagen synthesis of the cells was estimated by measuring the amount of Procollagen Type I C-peptide (PIP) levels in the medium with a commercially available ELISA kit (Panvera, Japan). Medium samples collected at the end of the experiment were diluted (1:9) and processed according to the manufacturer's instructions. PIP is a propeptide that is cleaved from the procollagen secreted by the cells and reflects the stoichiometric amount of collagen synthesized.

6.4 Results

Generally, free-floating FPCGs without TGF-β treatment, used for control, showed a moderate decrease in gel area from 0 to 12h, followed by a sharp reduction in gel area from 12h to 24h. From 24h to 48h, there was only a slight decrease in gel area. FPCGs treated with TGF-β3 contracted with a greater rate of gel area reduction from 0h to 12h. Further, TGF-β1 treatment resulted in a significant and steady reduction in gel area from 0h to 12h, before

approaching an equilibrium after 24h. Overall, both TGF-β1 and TGF-β3 treatments resulted in a significant reduction in gel area at 4, 8, 12, 24, and 48h compared to control gel area, but TGF-β1 caused a significantly greater reduction in gel area than TGF-β3 at 8, 12, 24, and 48h (**Figure 12**). Specifically, on average between 8 and 48 hours, the collagen gel area with TGF-β1 treatment was 25.5% smaller than that with TGF-β3 treatment. However, using the free-floating FPCG model, significant differences in the gel areas among the three dosages used (1, 5, and 25 ng/mL) could not be established for either TGF-β1 or TGF-β3.

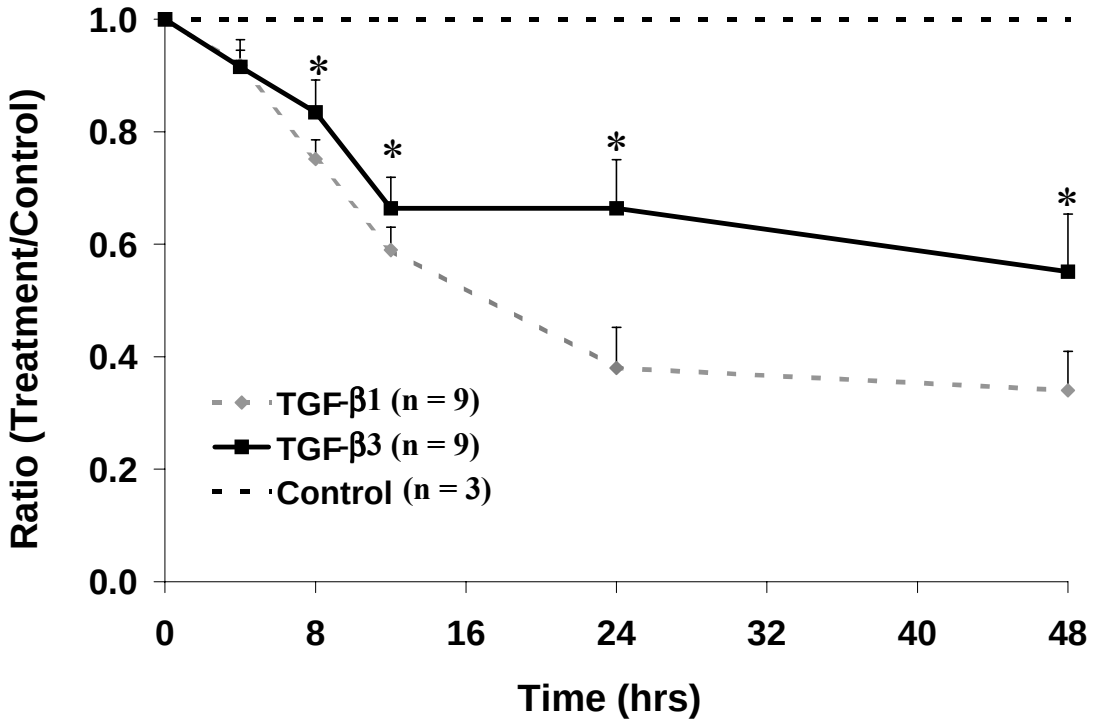

Figure 12 TGF-β3 induces less HPTF contraction of a free-floating FPCG compared to TGF-β1 at 8, 12, 24, and 48 hrs (* $p < 0.05$).

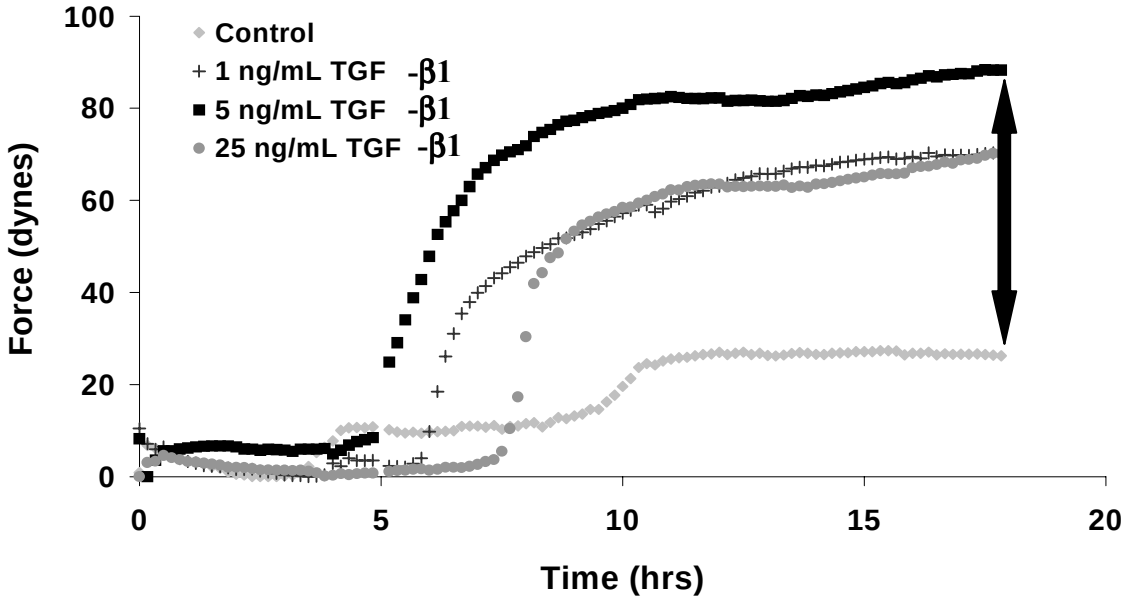

Figure 13 Using the CFM system, all dosages of TGF-β1 were found to increase the maximum contraction force of the HSFs in a collagen gel compared to non-treated controls. The 5 ng/mL of TGF-β1 resulted in the largest increase in maximum contraction force (360% of control; black arrow), whereas 1 and 25 ng/mL resulted in similar maximum contraction forces (280% of control).

Due to the inability of the free-floating FPCG model to detect the dose dependence of TGF-β1 and TGF-β3, the multi-station CFM system was used to monitor the effect of these growth factors on HSF contraction. Visually, the cells deformed the sides of the gel into a parabolic shape (**Figure 10)**, as a result of the near isometric tension in the FPCGs. The deformation of the FPCG from the sides of the silicone dish allow for the detection of contraction forces. Thus, any discrepancies in contraction forces measured by the CFM system may be attributed to the gel remaining attached to the silicone dish. In the first experiment, control FPCGs, with HSFs in serum-free medium without TGF-β treatment, resulted in minimal contraction (~20 dynes) after about 18h. However, HSFs treated with TGF-β1 (1, 5, and 25 ng/mL) caused a marked increase in maximum contraction force (45, 60, and 45 dynes,

respectively), as well as an earlier initiation of contraction (6.25, 5, and 7.5 h, respectively) (**Figure 13**). The contraction patterns for each of the TGF-β1 dosages are similar, with differences in initiation of the FPCG contraction and the maximum contraction force. Treatment with 5 ng/mL TGF-β1 resulted in the earliest initiation of contraction as well as the largest maximum force about 90 dynes (or 360% of control). In addition, treatment with 1 ng/mL of TGF-β1 resulted in an earlier increase in contraction compared with 25 ng/mL. Both dosages, however, resulted in about 70 dynes of maximum contraction force (280% of control) at 18h. Generally, a dose response to TGF-β1 treatment was observed, most noticeably affecting the initiation of contraction and the maximum force produced. Based on the MTT assay, the control, 1, 5, and 25 ng/mL TGF-β1 had similar cell activity (0.311, 0.373, 0.351, and 0.348 OD, respectively).

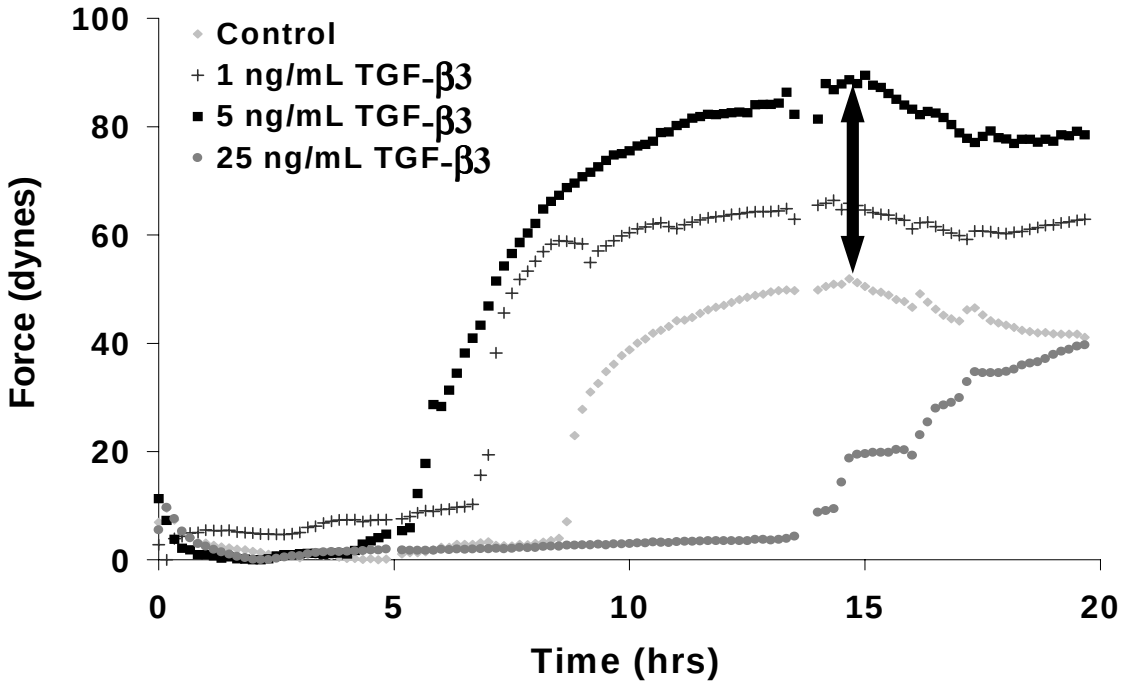

Figure 14 Using the CFM system, it was shown that TGF-β3 affected the initiation of contraction and the maximum force of contraction in a dose dependent manner. Specifically, similar to TGF-β1, 5 ng/mL of TGF-β3 resulted in the earliest contraction and the highest maximum contraction force (180% of control; black arrow).

Similar to TGF-β1, the dosages of TGF-β3 (1, 5, and 25 ng/mL) also affected the initiation of contraction (6.5, 5.2, and 13 h, respectively) and maximum contraction force produced (15, 40, and -10 dynes, respectively) (**Figure 14**). Further, treatment with 5 ng/mL TGF-β3 induced the earliest contraction (5.2h) and the highest maximum contraction force (180% of control) compared to the other dosages. Although 1 and 5 ng/mL TGF-β3 increased HSF contraction, 25 ng/mL TGF-β3 actually inhibited contraction by delaying the initiation of contraction and resulting in a lower maximum contraction force, 80% of control. The cell viability for the control, 1, 5, and 25 ng/mL TGF-β3 FPCGs were similar at the end of the experiment (0.233, 0.250, 0.268, and 0.265 OD, respectively).

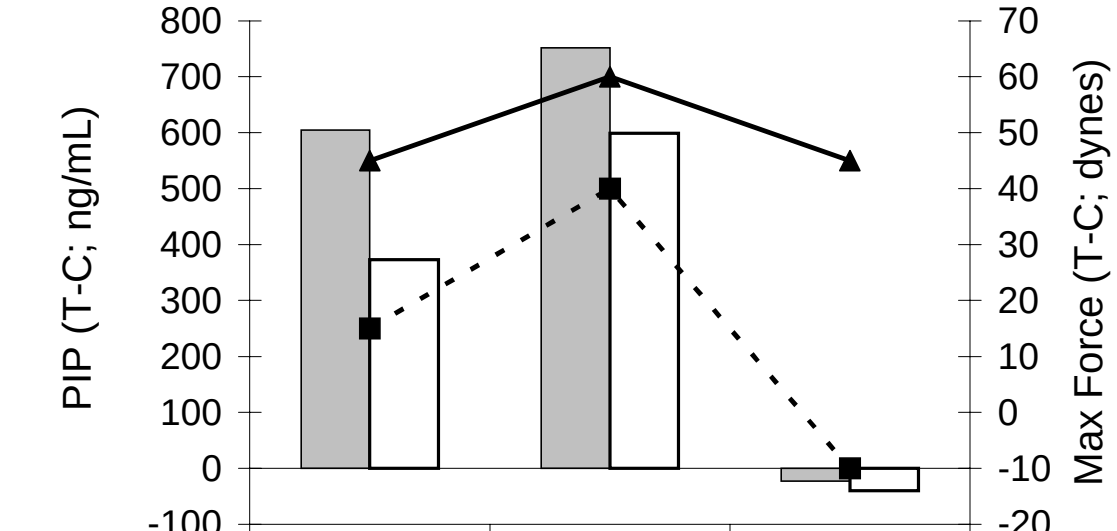

	1 ng/mL	5 ng/mL	25 ng/mL
PIP TGF-β1	605	752	-23
PIP TGF-β3	373	599	-40
Force TGF-β1	45	60	45
Force TGF-β3	15	40	-10

Figure 15 PIP levels (columns) and maximum contraction force (lines) are apparently dosage dependent for both TGF-β1 and TGF-β3. For both isoforms, the 5 ng/mL dose resulted in the largest increase in PIP levels and maximum contraction force. The trend for both collagen synthesis and maximum contraction force are similar for both isoforms, however, TGF-β3 increased PIP levels and maximum contraction force to a lesser degree than TGF-β1. (n = 1 for all dosages)

With the treatment of either TGF-β1 or TGF-β3, similar shapes of contraction patterns were observed. Also, although 5 ng/mL of both TGF-β1 and TGF-β3 resulted in the earliest contraction and the largest maximum contraction force compared to the other dosages, treatment with TGF-β1 caused about a 65 dyne increase in maximum contraction force (360% of control) compared to its respective non-treated control, whereas TGF-β3 resulted in only about a 40 dyne increase in contraction force (180% of control) compared to its non-treated control.

Furthermore, the amount of PIP in the medium at the end of the experiment was measured using an ELISA kit. It was found that the PIP levels followed a similar trend as the maximum contraction force for both TGF-β1 and TGF-β3, with 5 ng/mL of TGF-β treatment resulting in the largest PIP level increase, 752 and 599 ng/mL, respectively (**Figure 15**). The 25 ng/mL dosage for both TGF-β1 and TGF-β3 resulted in decreased PIP levels compared to control, -23 and -40 ng/mL respectively, whereas the 1 ng/mL TGF-β1 and TGF-β3 resulted in a 605 and 373 ng/mL increase in PIP levels compared to control.

Moreover, a similar dose dependent trend apparently exists between maximum contraction force and collagen synthesis. For both the maximum contraction force and PIP levels, the 5ng/mL dose for either TGF-β1 or TGF-β3 resulted in the largest increase compared to the other dosages. Further, for each dose, TGF-β1 treatment resulted in higher maximum contraction forces and PIP levels than TGF-β3. In addition, 25 ng/mL of TGF-β1 resulted in about a 45 dyne increase in maximum contraction force compared to its control, however, PIP levels apparently returned to the control values. In contrast, with 25 ng/mL of TGF-β3, both PIP levels and maximum contraction force returned to near control levels. Further, a strong relationship exists between the level of PIP and maximum contraction force (**Figure 16**).

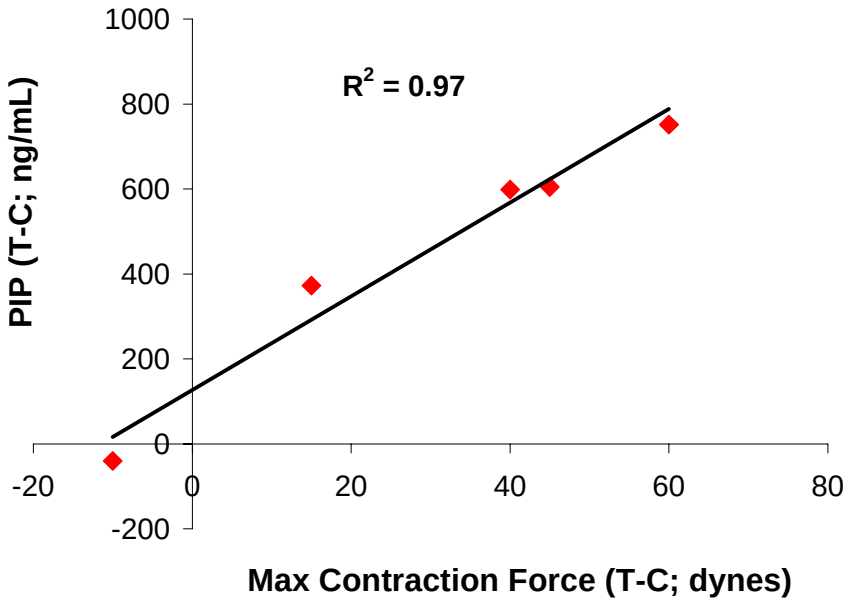

Figure 16 Collagen synthesis and cellular contraction have an apparently strong relationship since PIP levels and maximum contraction force appear to have a linear relationship.

6.5 Discussion

This study demonstrated that TGF-β1 and TGF-β3 treatments increase human fibroblast contraction in a collagen gel model, which is consistent with previous findings [18]. Moreover, this study quantify the effect of these growth factors on HSF contraction and indicate that TGF-β1 increases cellular contraction to a greater degree than TGF-β3. Although different systems were used to study cellular contraction, the HSFs and HPTFs responded similarly to the TGF-β1 and TGF-β3 treatments in that TGF-β3 resulted in less FPCG contraction than TGF-β1. Further, collagen synthesis, measured by PIP levels, followed a similar trend as the maximum contraction force, with apparent dose and isoform dependence. Moreover, collagen synthesis and cellular

contraction appear to have a strong relationship. In addition, it is worth discussing the variability of the controls for the TGF-β1 and TGF-β3 experiments, namely the different maximum contraction forces. Based on the OD value from the MTT experiment, the cell densities are similar within each experiment, but are different between the two experiments. This is most likely due to the controls being from two different experiments and the inherent variability in counting cells.

Cellular contraction is known to be an important component of connective tissue wound healing [12,26]. The finding that both TGF-β1 and TGF-β3 increase cellular contraction of a collagen gel supports previous studies using skin fibroblasts [18]. Moreover, this study differentiated between the contractile forces induced by TGF-β1 or TGF-β3 using two different methods, a free-floating FPCG and a multi-station CFM system. Although there were a limited number of samples, the effects of TGF-β1 and TGF-β3 were consistently demonstrated using two different models, as well as with fibroblasts from two different tissues. Since excessive contraction is proposed to result in scar tissue formation [26] and TGF-β1 results in larger cellular contraction and collagen synthesis compared with TGF-β3, this may help to explain why TGF-β1 induces scar formation whereas TGF-β3 reduces the formation of scar tissue [17].

In agreement with literature, TGF-β1 and TGF-β3 differentially increased collagen synthesis of human skin fibroblasts [18]. For healing tissues, each of these cellular responses plays an important role in the wound healing process. However, deviation from an optimal level for any of these cellular responses could adversely affect the quality and function of healing tissue. Therefore, as TGF-β1 was found to increase contraction and collagen synthesis of human skin

fibroblasts to a greater degree than TGF-β3, it is suggested that the lower cellular contraction and collagen synthesis induced by TGF-β3 may improve the quality of healing tissues.

Although these findings are preliminary and further studies are required, they are consistent with literature. Brown and coworkers also found that TGF-β1 and TGF-β3 were dose dependent, with moderate dosages (7.5 and 15 ng/mL) causing an optimal increase in human skin fibroblast contraction, whereas higher dosages (> 22.5 ng/mL) inhibited the cells' contraction [60]. Moreover, using both the free-floating FPCG and the CFM system, TGF-β1 consistently induced higher cellular contraction than TGF-β3. Since cellular responses potentially translate to the tissue level, the differential induction of cellular contraction and collagen synthesis by TGF-β1 and TGF-β3 suggested by our findings may explain the differential effects seen in healing tissues with treatment with these two isoforms.

7.0 SUMMARY AND FUTURE DIRECTIONS

The studies presented above are part of an overall objective, which is to reduce the formation of scar tissue by regulating cellular contraction. The first study demonstrated that HPTFs are contractile and that the cells' contraction depends on serum concentration. In that study, the TSM and FPCG models were used to demonstrate the cells' contraction, however these models were limited since they do not measure cellular contractile forces per se, and their sensitivity to detect small changes in cellular contraction forces is relatively low.

To overcome these shortcomings, a multi-station CFM system was developed that uses semi-conductor strain gages to monitor beam bending due to force produced by CPCGs. The current CFM system can measure four CPCGs simultaneously, which can be expanded for testing six CPCGs. The semi-conductor strain gages used on the beams increase the sensitivity of the system since the gage factor is three to four times greater than conventional gages, which are commonly used in the other systems. The multiple stations of this CFM system facilitate experimental designs and statistical analysis. With this CFM system, contractile forces of HPTFs and HSFs were measured. The results demonstrate that this system can differentiate between cells from different tissues by detecting differences in contraction patterns and maximum contraction force. This finding also suggests that regulation of cellular contraction may need to be tailored to the targeted cells, since cells from different tissues have different contractile patterns and may respond differently to the same treatments.

Using the CFM system, the effect of TGF-β1 and TGF-β3 on human fibroblast contraction was also studied. It was found that TGF-β1 induced higher cellular contraction force and collagen synthesis than TGF-β3. Further, both TGF-β1 and TGF-β3 were shown to be dose dependent, with 5 ng/mL for both isoforms resulting in the highest cellular contraction force and collagen synthesis. However, 25 ng/mL TGF-β1 caused a slight decrease in cellular contraction force but a substantial decrease in collagen synthesis compared to 5 ng/mL of TGF-β1, whereas 25 ng/mL TGF-β3 caused a substantial decrease in both cellular contraction force and collagen synthesis compared to 5 ng/mL of TGF-β3. Although future studies are underway to supplement these findings, certain dosages of TGF-β1 or TGF-β3 may be used to down-regulate fibroblast contraction and collagen synthesis and potentially reduce the formation of scar tissue.

In spite of all these interesting findings, a couple of limitations exist in these studies. First, normal fibroblasts were used in each of these studies; however, healing fibroblasts will probably have different cellular contraction and collagen synthesis compared to normal fibroblasts. To understand the differences between normal and healing fibroblasts, future studies will investigate the cellular contraction and collagen synthesis of healing fibroblasts with the CFM system. A second limitation is the use of cells from only a single donor for each experiment. On one hand, there is less variability when comparing between cells from the same donor; however, on the other hand, it remains to be established as to whether these effects are reproducible with cells from other donors. Future studies will use cells from different donors in an effort to supplement the existing data and demonstrate the reproducibility of these findings.

Several future studies are also underway to further investigate cellular contraction using this CFM system. One study is investigating the effect of prostaglandin E_2 (PGE_2), an inflammatory mediator of tendons [62], and hydrocortisone, which can reduce the formation of PGE_2, on HPTF contraction and collagen synthesis. The presence of PGE_2 in injured tendons, *e.g.* tendonitis, may affect the contraction of the tendon fibroblasts and the healing of the tendon. Preliminary data indicate that PGE_2 inhibits HPTF contraction of FF-FPCGs, whereas hydrocortisone increases HPTF contraction (**Figure 17 in the Appendix**). Thus, certain levels of PGE_2 may regulate tendon fibroblast contraction; however, if levels of PGE_2 are further elevated, this may further reduce tendon fibroblast contraction and impair the wound healing process. Understanding the effects of PGE_2 on cellular responses, *e.g.* cellular contraction and collagen synthesis, will help determine its role in tendon healing, as well as potential methods to regulate cellular contraction. The second study addresses a fundamental research question in our overall objective: Do healing fibroblasts contract more than normal fibroblasts? In fact, healing fibroblasts from rat medial collateral ligaments (MCLs) were found to contract to a greater degree than those from normal rat MCLs (**Figure 18 in the Appendix**). As the preliminary findings for both of these studies are encouraging, additional experiments will be performed to confirm these findings. Lastly, since the ratio of TGF-β1 and TGF-β3 is proposed to be important in regulating scar formation [59], a future study will investigate the combination of TGF-β1 and TGF-β3, in different ratios, on cellular contraction and collagen synthesis to understand the combined effect of these growth factors. Therefore, by regulating the degree of cellular contraction with treatments such as TGF-β3, formation of scar tissue in healing tissues, *i.e.* skin, tendons, and ligaments, may be reduced.

With the newly developed multi-station CFM system, there are many potential applications for future research investigating the role of cellular contraction in tissue wound healing. Using this system, contraction patterns of different cell types can be studied to determine how to optimally regulate the cells' contraction in order to reduce the formation of scar tissue. Although additional studies are needed, the findings in this thesis suggest that TGF-β3 may be used to regulate contraction and collagen synthesis of human skin and tendon fibroblasts, potentially reducing the formation of scar tissue. Moreover, the knowledge acquired by these studies can be used to investigate contraction of other cell types, such as endothelial cells, and determine the role of the cells in tissue healing.

Further, with use of the CFM system, future studies will focus on the healing mechanisms of tendons and ligaments, particularly focusing on the effect of growth factors, such as TGF-βs, platelet derived growth factor, endothelial growth factor, etc., on cellular contraction and collagen synthesis. However, the relationship of cellular contraction to other cellular responses important during wound healing, *i.e.* collagen synthesis, also remains to be investigated. These studies will help define the role of cellular contraction in tissue wound healing, and potentially lead to advanced treatments that target cellular contraction and subsequently improve the quality of healing tissue.

APPENDIX

Experimental Protocols

Preparation of TSMs

1. Hold a 25x25 mm (or 25x 50mm) cover slip with tweezers at one corner of the cover slip.
2. Use a scoop to place silicone (Wacker Silgel 601A) onto the top of the cover slip (spread the silicone over the entire cover slip, except for the corner where you are holding the cover slip, and don't use too much).
3. Turn the cover slip upside down, so that the silicone is on the bottom surface.
4. Hold it briefly over a bunsen burner flame (hold over the flame just long enough so that you see the surface glaze over, about 2 seconds).
5. Turn the cover slip right side up (with the silicone on the top surface).
6. Carefully place inside a petri dish without disrupting the membrane (if silicone flows out onto the petri dish, you will need to remake the TSM).
7. Place a small amount of Medical Adhesive Silicone Type onto the corner without any silicone (where you held the cover slip with the tweezers), being careful not to disrupt the membrane by touching it.
8. Leave the petri dish uncovered and expose the membrane to UV light for 1 hour.

Plating cells on TSMs

1. Make a fresh batch of pronectin.
2. Carefully pipette the pronectin to the side of the cover slip so that the pronetin gently overflows onto the silicone membrane.
3. Leave the pronectin sit on the membrane for ten minutes.
4. Extract the pronectin with a pipette, to the side of the cover slip.
5. Wash the membrane twice with PBS by the same overflow method used above (extract the PBS by the same means as above).
6. Cover the petri dishes and allow the membranes to dry before adding cells (place in incubator if necessary).
7. Count the cells and dilute to a cell concentration of $7x10^4$ cells/mL.
8. Add 1 mL of the $7x10^4$ cells/mL cell solution to the 25x50 cm^2 cover slip and 0.50 mL to the 25x25 cm^2 cover slip.
9. Incubate for 1 hour at 37^oC to allow cells to attach.
10. Check cell attachment.
11. Once cells are attached, add media so that the membrane is completely covered.
12. Place cells into 37^oC incubator and maintain cells.

Preparation of Free Floating-FPCGs

	Well Diameter 22 mm	
# of wells with gels:	33	
# of wells with cells:	30	
Desired cell density:	500,000 cells/mL	
Total growth media needed:	54.000 mL	
Total volume of cells needed:	9.000 mL	
Total collagen solution needed:	16.500 mL	
Total cell number:	4,500,000 cells	
Cell density:	395 cell/mm^2	
Collagen solution density:	2.560 mg/mL	

Cell Type: _____

Donor: _____

Passage used: _____

Date last split: _____

Initials: _____

GM: AIM-V media with 1% P/S

Collagen Solution

Add:	1.700 mL	10X PBS	
	1.700 mL	0.1 M NaOH	
	13.600 mL	Collagen Solution	3.2 mg/mL
Made:	17.000 mL		

Mix with pipette.
Check pH. Should be between 7.0 and 7.5 (a dark green color - see indicator).
pH indicator: _____

Place in refrigerator (time): _____

Keep refrigerated for at least 2 hours.

Collagen solution at Rm Temp: _____

Cell Preparation

Extract media.
Add 3 mL of trypsin to each dish.
Incubate for ~3 min. or until cells are detached.
Add 5 mL of DMEM (10% FBS, 1% P/S) per dish.
Pipette into conical tube.
Centrifuge at 1000 RPM for 5 min.
Extract supernatant.
Add GM to count cells.
Cell count (dilute to 500,000 cells/mL): _____

_____

Total volume needed: _____

Current volume: _____

Volume of GM to be added: _____

Seeding cells on collagen gel

To each well of an untreated 12-well plate add:

Well Diameter 22 mm		
0.300	mL	Cells (500,000 cells/mL)
0.500	mL	Collagen solution

Mix and remove bubbles.
Incubate at 37 C, 5% CO2 (for about 30 min).

Placed in incubator at: _____

After 30-45 minutes, to each well add:

Well Diameter 22 mm		
1.500	mL	GM (+condition)

Tap bottom of dish to detach gels

Returned to incubator at: _____

Measuring FPCG Contraction with the CFM System

1. Prepare incubator
    a. Fill water pan
    b. Clean CFM and shelves
    c. Make sure beam and tension unit attachments are set up properly
2. Check cells so that they are ~80% confluent
3. Clean and autoclave:
    a. Silicone dishes
    b. Gel attachment units
4. Warm medium and trypsin
5. Keep autoclaved parts (#3) in incubator to warm them to temperature
6. Make collagen gel solution, mix well, and place in 4°C until needed
    a. For 4 gels (mix in 50 ml conical tube):
        i. 2.2 ml of 10x PBS
        ii. 2.2 ml of 0.1 M NaOH
        iii. 17.4 ml collagen stock solution (Vitrogen, 0701 FXP-019)
7. Setup computer and data acquisition system
    a. Turn on power supply and check excitation voltage with volt meter (this will allow strain gages to get to temperature)
    b. Open CFM experiment and CFM set-up programs
    c. Change path to "C:\WINDOWS\Desktop\CFM [cell type] [date].txt", *i.e.* "C:\WINDOWS\Desktop\CFM HPTF 032402.txt"
8. Prepare cells:
    a. Extract medium from petri dish
    b. Add 3 ml of trypsin to cells and place in incubator for about 2 minutes
    c. Check cells, via light microscope, to ensure that they are unattached (tapping the bottom of the petri dish can loosen some cells as well)
    d. Add 5 ml of growth medium (with 10% FBS) to counter the trypsin
    e. Using a pipette, tilt the petri dish and wash cells to the bottom
    f. Pipette the cells into an appropriate sized conical tube (15 or 50 ml)
    g. Centrifuge the cell solution (1000 RPM for 5 minutes); prepare hemacytometer while waiting for the centrifuge
    h. Extract the supernatant, leaving the cell pellet and a small amount of solution, try not to loose cells
    i. Add a small amount of the medium that will be used in the experiment, depending on the desired density, and mix well

j. Count cells with hemacytometer
    i. Clean and dry hemacytometer
    ii. Place cover slip on hemacytometer
    iii. Obtain 10 µl of well mixed cell solution and pipette onto hemacytometer
    iv. Count the four corners and find the total number of cells per ml=$(C_1+C_2+C_3+C_4)x10^4/4$ (cells/ml)
    v. Dilute cell solution to appropriate density
9. Set out collagen solution while waiting for the centrifuge
10. Prepare dishes and gel attachment units so that FPCG solution can be added
11. Mix:
    a. Desired cell density 66.66 (=$2x10^6$ cells/gel)
    b. 13.2 ml cells to the 22 ml collagen
12. Pipet 8 ml of mixture into silicone dish and between vyon bars
13. Incubate for 10 minutes
    a. While waiting, start CFM program on computer
14. Add 7ml of appropriate growth medium (AIM-V with TGF-β1 or 3)
15. Label gels
16. Attach to CFM and provide initial tension (check by seeing ~2-3mV increase)
17. Make sure everything is running properly and clean up
    a. Properly dispose of all used materials, including cells, into biohazard waste receptacle
    b. Wash hood down with ethanol
    c. Clean hemacytometer and cover slip with ethanol
18. Obtain 100 µl of medium from each sample for the procollagen assay
19. Let experiment run for the designated time
20. Collect 100 µl of medium at the end of the experiment
21. Perform MTT assay
    a. Note: after 3h incubation, use chemidoc system to take pictures of the contracted gels

Measuring Cell Viability with MTT Assay

For FF-FPCG:

1. Add 200 µL MTT solution to each FF-FPCG
2. Incubate for 3h
3. Centrifuge plate of FF-FPCG 1900 RPM for 5 minutes
4. Remove supernatant
5. Add 2 mL extraction buffer
6. Incubate overnight
7. Add 20 mL DI H_2O (1:5 dilution)
8. Add 200 µL to 96 well plate (run in duplicates)
9. Read plate at 550 nm using microplate reader (SpectraMax 190, Molecular Devices)

For FPCG in the CFM System:

1. Add 500 µL MTT solution to each FPCG (leave attached to CFM)
2. Incubate for 3h
3. Detach FPCG from CFM
4. Transfer FPCG to 50 mL conical tube
5. Centrifuge 1900 RPM for 5 minutes
6. Remove supernatant
7. Add 4 mL extraction buffer
8. Incubate overnight
9. Add 20 mL DI H_2O (1:5 dilution)
10. Vortex
11. Add 200 µL to 96 well plate (run in duplicates)
12. Read plate at 550 nm

Multi-Station CFM System: Parts List

Item	Description	Vendor	Catalog #	Price/ea
Semi-conductor strain gages	Mounted on beams to measure beam bending	Micron Instruments	G150786	$160.60
Support rod	Hard aluminum rod-12" long, 0.5" diam	Fisher Scientific	14-666-10G	$7.55
Support rod	Hard aluminum rod – 18" long, 0.5" diam	Fisher Scientific	14-666-10B	$8.78
Rod Connectors	90° angle, 0.5" hole, castaloy metal	Fisher Scientific	14-666-20	$6.93
CFM base and fixation units	Aluminum base/fixation units and 25 hours of labor	School of Engineering Machine Shop		$854.50
Beam clamps	Stainless steel beam clamps (4) and 5 hours of labor	School of Engineering Machine Shop		$165.75
Strain gage wire	100' wire to wire gages to connector block	Measurements Group	426-DFV	
Wire frames (gel attachment units)	0.014" diameter wire, Stainless steel type 304 V wire	Small Parts.com	U-SWGX-140	$1.70
DAQ card – 6024E	PCMCIA DAQ card with digital triggering, two analog outputs, two counter/timers, eight digital I/O lines	National Instruments	778269-01	$625.50
Shielded cable	Cable for connecting to connector block	National Instruments	186838-02	$99.00
Shielded connector block	Block connecting CFM and voltage source (SCB-68)	National Instruments	776844-01	$265.50
IBM 2628 notebook	550 MHz/6GB/64MB/12.1" TFT/Win98	TigerDirect.com	M975-26281UU	$799.99
Vyon bars	Attachment area for the gel	Porvair, Inc.		Sample
Silicone dishes	Cells and collagen gels placed inside			Made in the lab

Data Acquisition Program (Labview 5.1) for Monitoring Cellular Contraction

Summary: Program overview

The LabView program for the CFM was designed to display and record the signal voltage from the semiconductor strain gages. Further, the user can define the number of data points sampled, as well as the time interval over which the data points are collected. This program consists of a combination of "for loops" and "while loops" with sequence structure frames used to separate the data acquisition program and the delay. **For Loop A** allows the user to specify the number of times the entire program runs before stopping. The program is set to run 200,000,000 times, an arbitrarily large number so that the user is able to end the program at the end of the experiment before the program terminates itself. Within the first sequence structure, **Frame 1**, **For Loop B** allows the user to specify the number of data points to be recorded per run through the program. The portion of the program that records the voltage signal from the strain gages is located in While Loop C. This allows for the continual running and specification of the sampling rate for recording the data. The next frame in the sequence structure, **Frame 2**, contains the program delay. This delay is user specified on the data screen in minutes, default delay set to 10 minutes. When the data is recorded from the system, it is automatically saved to the user specified location in the Microsoft Excel format (*.xls). The user is also able to input the upper and lower voltage limits on the front panel, which can change the resolution of the data acquisition system, therefore, it should usually be left at the default setting. The program is designed to record as many as eight channels at a time (1 channel/bar); however, only those channels specified are recorded. The default setting for the program is to use Device 1 and record channels 1, 2, 3, and 4.

Code Descriptions: Code used in the program

1. **Sequence Structure –** This function allows for the recording of data from the strain gage in **Frame 1** followed by a delay in **Frame 2**.

2. **For Loop(s) -** Two "for loops" exist in the program. The outermost "for loop, " **For Loop A**, allows the user to specify the number of times the program should run through the entire program. The second "for loop, " **For Loop B**, allows the user to specify the number of times **Frame 1** should run before continuing to **Frame 2** for the delay. The default value of the outermost "for loop" is currently 200,000,000, an arbitrary large number so that the program may run continuously until user manually stops the program,

and the default value for the innermost "for loop" is 100 iterations which corresponds to the number of samples taken each time through the program. The user is able to define the number of iterations that are desired at each time point.

3. **While Loop –** The "while loop," **While Loop C**, allows the program in **Frame 1** to run continuously for the number of specified times in the "for loop." After each run through the "while loop," the signal voltage is recorded.

4. **High/Low Limits –** These are the limits that the program has set when recording the data. The user is able to specify these numbers on the front panel of the program. The default setting is a low limit of 0.0 and a high limit of 0.01. Changing these values will change the gain of the data acquisition card.

5. **Delay Timer –** The delay in **Frame 2** of the sequence structure is set up to take the user input time delay value from the front panel of the diagram and multiply it by 60000 to convert the entered minute value into milliseconds. The delay is not 100% accurate. The delay can be slightly more or less than the specified time in milliseconds. This discrepancy does not affect the overall value of the delay, however, since the value varies on a millisecond level.

6. **Time Stamp –** As each data point is recorded, the time that the data point is recorded is also saved in another sheet that the user is able to specify.

7. **Save to File Function –** This function allows the user to save the data that is read to a specified file on the computer. The True/False statement included with this function tells the program to add each subsequent data point to those previously recorded without writing over the data points. The statement should always be true in order to record without writing over the previous data. The user is able to specify where the data will be saved on the front panel of diagram. The current default setting is for the data to be saved as a Microsoft Excel file on the computer desktop with the file name being test. An example of the name appearing on the front panel is C:Window/Desktop/test.xls. The default setting is currently at three decimal places for each data point. The setting for the decimal places can be changed by adjusting the numeric value associated with the function located as a numeric constant wired to the function.

8. **Analog Input –** This function records the signal read by the channels specified by the user on the front panel of the diagram. This function in particular, allows "for loop" iterations to record multiple data over a period of time, as well as the specification of various other aspects. The data is recorded as 1D array, which is then saved to the hard disk and graphed on the front panel. The high and low input limits are specified allowing for more precision in the answer.

9. **Array to Graph –** With the data being continuously recorded, it is important to see the general trend that is occurring through each iteration of the frame. Only those channels, which are specified, are plotted on the graph, and each channel is plotted as a different color. The current values that are being recorded are also placed next to the graph in a

table format with a precision of three decimal places. The recorded value from the analog input function is multiplied by 1000. This allows for the conversion of volts to millivolts for easier numbers to work with for the experiment.

Program Functions: Understanding the code

1. **Channel Monitoring –** The embedded program/sub VI, channel name to string array, was designed for the specific purpose of monitoring the specified channels.

2. **Time Stamp –** Defines the time at which each sample was taken for reference.

3. **Delay –** In order to obtain a delay in the program, a sequence structure is used. With this structure, the program is unable to go from **Frame 1** to **Frame 2** without first completing the desired number of iterations in **Frame 1**. **Frame 2** holds the delay portion of the program. LabView has a "wait" function available that counts in milliseconds. This function was easily used for the program by incorporating a multiplication factor in order to change the delay time in minutes to milliseconds for the function to understand. When the time is changed from minutes to milliseconds, some discrepancy may arise, but the discrepancy will be in milliseconds making any difference inconsequential to the delay time.

4. **Inputs –**There are a number of user specified inputs on the front panel. The following lists each individual input, its function, and default value.

    - Device – The default value is set to 1. This is a constant numeric value because the device is always located at 1. If multiple devices are used by the same computer there may then be other device numbers.
    - Voltage Limits – Both the High and Low voltage limits are input by the user. These limits set the gain of the strain gages adjusting the resolution of the voltage recorded. The default values are 0.00 and 0.10 for the low and high limits, respectively.
    - Channels – These are the channels that are reading the voltages from the stain gages. The default values are 1, 2, 3, and 4. The program can record up to 8 channels in the differential mode. Provided that the proper wires are connected to the proper channels, any 4 channels could be chosen. In this experiment, the wires are connected to the four previously specified channels.
    - Sampling Rate – This refers to the number of samples taken for a given time frame. The sampling rate is set at 10 sample/ 1 sec, i.e. 10 Hz. This value allows the user to take 100 samples every 10 seconds, the desired number of samples for this project.

- Delay – This value was discussed above. As stated above the input value is entered as the number of minutes the program should delay. The default value is set to 10 minutes.

PGE_2 Reduces whereas Hydrocortisone Increases HPTF Contraction of a Collagen Gel

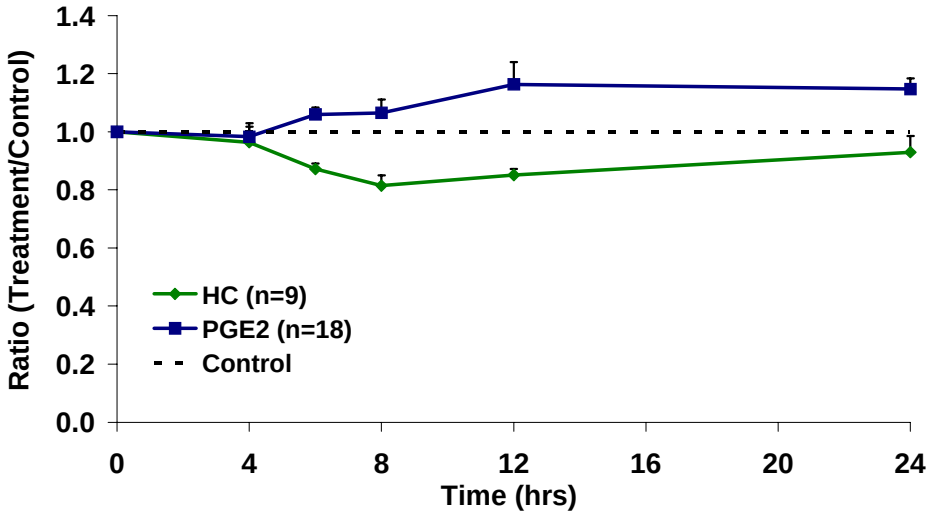

Figure 17 PGE_2 significantly inhibited HPTF contraction of a collagen gel at 6, 8, 12, and 24h compared with untreated controls and treatment with hydrocortisone (HC).

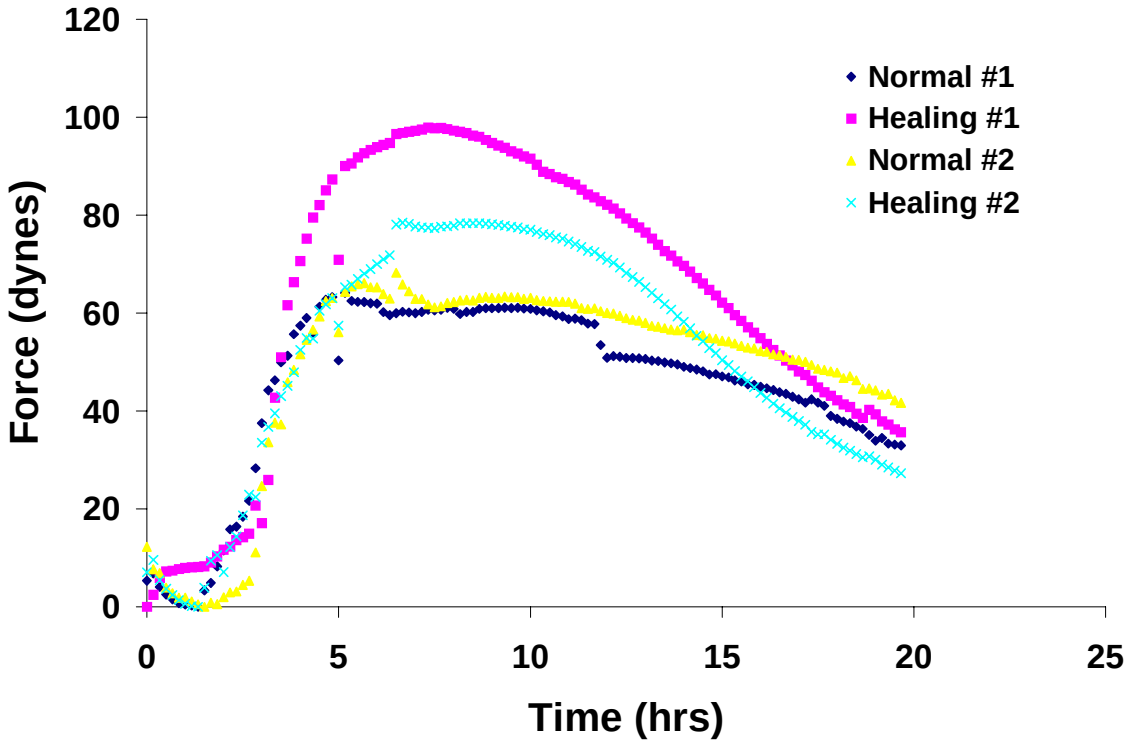

Figure 18 Healing and normal rat MCL fibroblasts have similar initial contraction rates, however, the healing fibroblasts contract with a greater maximum force than the normal fibroblasts.

BIBLIOGRAPHY

BIBLIOGRAPHY

1. Clark, J. A., Cheng, J. C. and Leung, K. S., "Mechanical Properties of Normal Skin and Hypertrophic Scars," Burns, Vol. 22, No.6 (1996), pp. 443-6.

2. Berry, D. P., Harding, K. G., Stanton, M. R., Jasani, B. and Ehrlich, H. P., "Human Wound Contraction: Collagen Organization, Fibroblasts, and Myofibroblasts," Plast Reconstr Surg, Vol. 102, No.1 (1998), pp. 124-31; discussion 132-4.

3. Gigante, A., Specchia, N., Rapali, S., Ventura, A. and de Palma, L., "Fibrillogenesis in Tendon Healing: An Experimental Study," Boll Soc Ital Biol Sper, Vol. 72, No.7-8 (1996), pp. 203-10.

4. Lawrence, W. T., "Physiology of the Acute Wound," Clin Plast Surg, Vol. 25, No.3 (1998), pp. 321-40.

5. Milano, G., Gigante, A., Panni, A. S., Mulas, P. D. and Fabbriciani, C., "Patellar Tendon Healing after Removal of Its Central Third. A Morphologic Evaluation in Rabbits," Knee Surg Sports Traumatol Arthrosc, Vol. 9, No.2 (2001), pp. 92-101.

6. Rockwell, W. B., Cohen, I. K. and Ehrlich, H. P., "Keloids and Hypertrophic Scars: A Comprehensive Review," Plast Reconstr Surg, Vol. 84, No.5 (1989), pp. 827-37.

7. Reddy, G. K., Stehno-Bittel, L. and Enwemeka, C. S., "Matrix Remodeling in Healing Rabbit Achilles Tendon," Wound Repair Regen, Vol. 7, No.6 (1999), pp. 518-27.

8. Longaker, M. T., Whitby, D. J., Ferguson, M. W., Harrison, M. R., Crombleholme, T. M., Langer, J. C., Cochrum, K. C., Verrier, E. D. and Stern, R., "Studies in Fetal Wound Healing: Iii. Early Deposition of Fibronectin Distinguishes Fetal from Adult Wound Healing," J Pediatr Surg, Vol. 24, No.8 (1989), pp. 799-805.

9. Longaker, M. T., Whitby, D. J., Adzick, N. S., Crombleholme, T. M., Langer, J. C., Duncan, B. W., Bradley, S. M., Stern, R., Ferguson, M. W. and Harrison, M. R., "Studies in Fetal Wound Healing, Vi. Second and Early Third Trimester Fetal Wounds Demonstrate Rapid Collagen Deposition without Scar Formation," J Pediatr Surg, Vol. 25, No.1 (1990), pp. 63-8; discussion 68-9.

10. Whitby, D. J., Longaker, M. T., Harrison, M. R., Adzick, N. S. and Ferguson, M. W., "Rapid Epithelialisation of Fetal Wounds Is Associated with the Early Deposition of Tenascin," J Cell Sci, Vol. 99, No.Pt 3 (1991), pp. 583-6.

11. Adzick, N. S. and Lorenz, H. P., "Cells, Matrix, Growth Factors, and the Surgeon. The Biology of Scarless Fetal Wound Repair," Ann Surg, Vol. 220, No.1 (1994), pp. 10-8.

12. Coleman, C., Tuan, T. L., Buckley, S., Anderson, K. D. and Warburton, D., "Contractility, Transforming Growth Factor-Beta, and Plasmin in Fetal Skin Fibroblasts: Role in Scarless Wound Healing," Pediatr Res, Vol. 43, No.3 (1998), pp. 403-9.

13. Burton, K. and Taylor, D. L., "Traction Forces of Cytokinesis Measured with Optically Modified Elastic Substrata," Nature, Vol. 385, No.6615 (1997), pp. 450-4.

14. Eastwood, M., Porter, R., Khan, U., McGrouther, G. and Brown, R., "Quantitative Analysis of Collagen Gel Contractile Forces Generated by Dermal Fibroblasts and the Relationship to Cell Morphology," J Cell Physiol, Vol. 166, No.1 (1996), pp. 33-42.

15. Khan, U., Occleston, N. L., Khaw, P. T. and McGrouther, D. A., "Differences in Proliferative Rate and Collagen Lattice Contraction between Endotenon and Synovial Fibroblasts," J Hand Surg [Am], Vol. 23, No.2 (1998), pp. 266-73.

16. Torres, D. S., Freyman, T. M., Yannas, I. V. and Spector, M., "Tendon Cell Contraction of Collagen-Gag Matrices in Vitro: Effect of Cross-Linking," Biomaterials, Vol. 21, No.15 (2000), pp. 1607-19.

17. Shah, M., Foreman, D. M. and Ferguson, M. W., "Neutralisation of Tgf-Beta 1 and Tgf-Beta 2 or Exogenous Addition of Tgf-Beta 3 to Cutaneous Rat Wounds Reduces Scarring," J Cell Sci, Vol. 108, No.Pt 3 (1995), pp. 985-1002.

18. Murata, H., Zhou, L., Ochoa, S., Hasan, A., Badiavas, E. and Falanga, V., "Tgf-Beta3 Stimulates and Regulates Collagen Synthesis through Tgf-Beta1- Dependent and Independent Mechanisms," J Invest Dermatol, Vol. 108, No.3 (1997), pp. 258-62.

19. Chang, J., Thunder, R., Most, D., Longaker, M. T. and Lineaweaver, W. C., "Studies in Flexor Tendon Wound Healing: Neutralizing Antibody to Tgf-Beta1 Increases Postoperative Range of Motion," Plast Reconstr Surg, Vol. 105, No.1 (2000), pp. 148-55.

20. Krummel, T. M., Michna, B. A., Thomas, B. L., Sporn, M. B., Nelson, J. M., Salzberg, A. M., Cohen, I. K. and Diegelmann, R. F., "Transforming Growth Factor Beta (Tgf-Beta) Induces Fibrosis in a Fetal Wound Model," Journal of Pediatric Surgery, Vol. 23, No.7 (1988), pp. 647-52.

21. Sullivan, K. M., Lorenz, H. P., Meuli, M., Lin, R. Y. and Adzick, N. S., "A Model of Scarless Human Fetal Wound Repair Is Deficient in Transforming Growth Factor Beta," Journal of Pediatric Surgery, Vol. 30, No.2 (1995), pp. 198-202; discussion 202-3.

22. Martin, P., "Wound Healing--Aiming for Perfect Skin Regeneration," Science, Vol. 276, No.5309 (1997), pp. 75-81.

23. Nodder, S. and Martin, P., "Wound Healing in Embryos: A Review," Anat Embryol (Berl), Vol. 195, No.3 (1997), pp. 215-28.

24. al-Qattan, M. M., Posnick, J. C., Lin, K. Y. and Thorner, P., "Fetal Tendon Healing: Development of an Experimental Model," Plast Reconstr Surg, Vol. 92, No.6 (1993), pp. 1155-60; discussion 1161.

25. Cox, D. A., "Transforming Growth Factor-Beta 3," Cell Biol Int, Vol. 19, No.5 (1995), pp. 357-71.

26. Nedelec, B., Ghahary, A., Scott, P. G. and Tredget, E. E., "Control of Wound Contraction. Basic and Clinical Features," Hand Clin, Vol. 16, No.2 (2000), pp. 289-302.

27. Khan, U., Kakar, S., Akali, A., Bentley, G. and McGrouther, D. A., "Modulation of the Formation of Adhesions During the Healing of Injured Tendons," J Bone Joint Surg Br, Vol. 82, No.7 (2000), pp. 1054-8.

28. Ngo, M., Pham, H., Longaker, M. T. and Chang, J., "Differential Expression of Transforming Growth Factor-Beta Receptors in a Rabbit Zone Ii Flexor Tendon Wound Healing Model," Plast Reconstr Surg, Vol. 108, No.5 (2001), pp. 1260-7.

29. Kolodney, M. S. and Wysolmerski, R. B., "Isometric Contraction by Fibroblasts and Endothelial Cells in Tissue Culture: A Quantitative Study," Journal of Cell Biology, Vol. 117, No.1 (1992), pp. 73-82.

30. Takayama, Y. and Mizumachi, K., "Effects of Lactoferrin on Collagen Gel Contractile Activity and Myosin Light Chain Phosphorylation in Human Fibroblasts," FEBS Lett, Vol. 508, No.1 (2001), pp. 111-6.

31. Chrzanowska-Wodnicka, M. and Burridge, K., "Rho-Stimulated Contractility Drives the Formation of Stress Fibers and Focal Adhesions," J Cell Biol, Vol. 133, No.6 (1996), pp. 1403-15.

32. Stopak, D. and Harris, A. K., "Connective Tissue Morphogenesis by Fibroblast Traction. I. Tissue Culture Observations," Dev Biol, Vol. 90, No.2 (1982), pp. 383-98.

33. Ehrlich, H. P. and Rajaratnam, J. B., "Cell Locomotion Forces Versus Cell Contraction Forces for Collagen Lattice Contraction: An in Vitro Model of Wound Contraction," Tissue Cell, Vol. 22, No.4 (1990), pp. 407-17.

34. Gabbiani, G., Hirschel, B. J., Ryan, G. B., Statkov, P. R. and Majno, G., "Granulation Tissue as a Contractile Organ. A Study of Structure and Function," J Exp Med, Vol. 135, No.4 (1972), pp. 719-34.

35. Coulomb, B., Dubertret, L., Bell, E. and Touraine, R., "The Contractility of Fibroblasts in a Collagen Lattice Is Reduced by Corticosteroids," J Invest Dermatol, Vol. 82, No.4 (1984), pp. 341-4.

36. Delvoye, P., Wiliquet, P., Leveque, J. L., Nusgens, B. V. and Lapiere, C. M., "Measurement of Mechanical Forces Generated by Skin Fibroblasts Embedded in a Three-Dimensional Collagen Gel," J Invest Dermatol, Vol. 97, No.5 (1991), pp. 898-902.

37. Eastwood, M., McGrouther, D. A. and Brown, R. A., "A Culture Force Monitor for Measurement of Contraction Forces Generated in Human Dermal Fibroblast Cultures: Evidence for Cell-Matrix Mechanical Signalling," Biochim Biophys Acta, Vol. 1201, No.2 (1994), pp. 186-92.

38. Khan, U., Occleston, N. L., Khaw, P. T. and McGrouther, D. A., "Single Exposures to 5-Fluorouracil: A Possible Mode of Targeted Therapy to Reduce Contractile Scarring in the Injured Tendon," Plast Reconstr Surg, Vol. 99, No.2 (1997), pp. 465-71.

39. Grinnell, F., "Fibroblasts, Myofibroblasts, and Wound Contraction," J Cell Biol, Vol. 124, No.4 (1994), pp. 401-4.

40. Harris, A. K., Wild, P. and Stopak, D., "Silicone Rubber Substrata: A New Wrinkle in the Study of Cell Locomotion," Science, Vol. 208, No.4440 (1980), pp. 177-9.

41. Bell, E., Ivarsson, B. and Merrill, C., "Production of a Tissue-Like Structure by Contraction of Collagen Lattices by Human Fibroblasts of Different Proliferative Potential in Vitro," Proc Natl Acad Sci U S A, Vol. 76, No.3 (1979), pp. 1274-8.

42. Orthopaedic Research Society, Dallas, TX, 2002, "Tgf-Beta1 and Tgf-Beta3 Differentially Induce Contraction of Human Tendon Fibroblasts: Implication of Improving the Quality of Healing Tendons, by Campbell, B. H. and Wang, J. H.-C." (2002), pp.

43. Freyman, T. M., Yannas, I. V., Yokoo, R. and Gibson, L. J., "Fibroblast Contraction of a Collagen-Gag Matrix," Biomaterials, Vol. 22, No.21 (2001), pp. 2883-91.

44. Nakagawa, S., Pawelek, P. and Grinnell, F., "Long-Term Culture of Fibroblasts in Contracted Collagen Gels: Effects on Cell Growth and Biosynthetic Activity," J Invest Dermatol, Vol. 93, No.6 (1989), pp. 792-8.

45. Unemori, E. N. and Werb, Z., "Reorganization of Polymerized Actin: A Possible Trigger for Induction of Procollagenase in Fibroblasts Cultured in and on Collagen Gels," J Cell Biol, Vol. 103, No.3 (1986), pp. 1021-31.

46. Allenberg, M., Weinstein, T., Li, I. and Silverman, M., "Activation of Procollagenase Iv by Cytochalasin D and Concanavalin a in Cultured Rat Mesangial Cells: Linkage to Cytoskeletal Reorganization," J Am Soc Nephrol, Vol. 4, No.10 (1994), pp. 1760-70.

47. Cowin, A. J., Holmes, T. M., Brosnan, P. and Ferguson, M. W., "Expression of Tgf-Beta and Its Receptors in Murine Fetal and Adult Dermal Wounds," Eur J Dermatol, Vol. 11, No.5 (2001), pp. 424-31.

48. Boemi, L., Allison, G. M., Graham, W. P., Krummel, T. M. and Ehrlich, H. P., "Differences between Scar and Dermal Cultured Fibroblasts Derived from a Patient with Recurrent Abdominal Incision Wound Herniation," Plast Reconstr Surg, Vol. 104, No.5 (1999), pp. 1397-405.

49. Khouw, I. M., van Wachem, P. B., Plantinga, J. A., Vujaskovic, Z., Wissink, M. J., de Leij, L. F. and van Luyn, M. J., "Tgf-Beta and Bfgf Affect the Differentiation of Proliferating Porcine Fibroblasts into Myofibroblasts in Vitro," Biomaterials, Vol. 20, No.19 (1999), pp. 1815-22.

50. Skold, C. M., Liu, X. D., Zhu, Y. K., Umino, T., Takigawa, K., Ohkuni, Y., Ertl, R. F., Spurzem, J. R., Romberger, D. J., Brattsand, R. and Rennard, S. I., "Glucocorticoids Augment Fibroblast-Mediated Contraction of Collagen Gels by Inhibition of Endogenous Pge Production," Proc Assoc Am Physicians, Vol. 111, No.3 (1999), pp. 249-58.

51. Smith, P., Mosiello, G., Deluca, L., Ko, F., Maggi, S. and Robson, M. C., "Tgf-Beta2 Activates Proliferative Scar Fibroblasts," J Surg Res, Vol. 82, No.2 (1999), pp. 319-23.

52. Ehrlich, H. P., Gabbiani, G. and Meda, P., "Cell Coupling Modulates the Contraction of Fibroblast-Populated Collagen Lattices," J Cell Physiol, Vol. 184, No.1 (2000), pp. 86-92.

53. Varedi, M., Tredget, E. E., Ghahary, A. and Scott, P. G., "Stress-Relaxation and Contraction of a Collagen Matrix Induces Expression of Tgf-Beta and Triggers Apoptosis in Dermal Fibroblasts," Biochem Cell Biol, Vol. 78, No.4 (2000), pp. 427-36.

54. Ballas, C. B. and Davidson, J. M., "Delayed Wound Healing in Aged Rats Is Associated with Increased Collagen Gel Remodeling and Contraction by Skin Fibroblasts, Not with Differences in Apoptotic or Myofibroblast Cell Populations," Wound Repair Regen, Vol. 9, No.3 (2001), pp. 223-37.

55. Katoh, K., Kano, Y., Amano, M., Kaibuchi, K. and Fujiwara, K., "Stress Fiber Organization Regulated by Mlck and Rho-Kinase in Cultured Human Fibroblasts," Am J Physiol Cell Physiol, Vol. 280, No.6 (2001), pp. C1669-79.

56. Levinson, H., Peled, Z., Liu, W., Longaker, M. T., Allison, G. M. and Ehrlich, H. P., "Fetal Rat Amniotic Fluid: Transforming Growth Factor Beta and Fibroblast Collagen Lattice Contraction," J Surg Res, Vol. 100, No.2 (2001), pp. 205-10.

57. Jacobs, D., Martens, M., Van Audekercke, R., Mulier, J. C. and Mulier, F., "Comparison of Conservative and Operative Treatment of Achilles Tendon Rupture," Am J Sports Med, Vol. 6, No.3 (1978), pp. 107-11.

58. Wang, J. H. and Grood, E. S., "The Strain Magnitude and Contact Guidance Determine Orientation Response of Fibroblasts to Cyclic Substrate Strains," Connect Tissue Res, Vol. 41, No.1 (2000), pp. 29-36.

59. Shah, M., Revis, D., Herrick, S., Baillie, R., Thorgeirson, S., Ferguson, M. and Roberts, A., "Role of Elevated Plasma Transforming Growth Factor-Beta1 Levels in Wound Healing," Am J Pathol, Vol. 154, No.4 (1999), pp. 1115-24.

60. Brown, R. A., Sethi, K. K., Gwanmesia, I., Raemdonck, D., Eastwood, M. and Mudera, V., "Enhanced Fibroblast Contraction of 3d Collagen Lattices and Integrin Expression by Tgf-Beta1 and -Beta3: Mechanoregulatory Growth Factors?," Exp Cell Res, Vol. 274, No.2 (2002), pp. 310-22.

61. Voytik-Harbin, S. L., Brightman, A. O., Waisner, B., Lamar, C. H. and Badylak, S. F., "Application and Evaluation of the Alamarblue Assay for Cell Growth and Survival of Fibroblasts," In Vitro Cell Dev Biol Anim, Vol. 34, No.3 (1998), pp. 239-46.

62. Almekinders, L. C., Baynes, A. J. and Bracey, L. W., "An in Vitro Investigation into the Effects of Repetitive Motion and Nonsteroidal Antiinflammatory Medication on Human Tendon Fibroblasts," Am J Sports Med, Vol. 23, No.1 (1995), pp. 119-23.